Deletion of core septin gene *aspB* in *Aspergillus fumigatus* results in fungicidal activity of caspofungin

Rebecca Jean Busch[1], Carson Doty[2], C. Allie Mills[3], Flutur Latifi[4], Laura E. Herring[3], Vjollca Konjufca[4], and José M Vargas-Muñiz[1,5,6*]

[1]Department of Biological Sciences, Virginia Tech, Blacksburg, Virginia, United States

[2]School of Biological Sciences, Southern Illinois University-Carbondale, Carbondale, Illinois, United States

[3]Michael Hooker Metabolomics and Proteomics Core Facility, Department of Pharmacology, University of North Carolina at Chapel Hill, Chapel Hill, North Carolina, United States

[4]Microbiology Program, Southern Illinois University-Carbondale, Carbondale, Illinois, United States

[5]Fralin Life Science Institute, Virginia Tech, Blacksburg, VA

[6]Center for Emerging, Zoonotic, and Arthropod-borne Pathogens, Virginia Tech, Blacksburg, VA

Running title: Septin response to caspofungin

* Corresponding author

E-mail: j.vargas.muniz@vt.edu (JVM)

Abstract:

Septins are a family of GTP-binding proteins found in many eukaryotic lineages. Although highly conserved throughout many eukaryotes, their functions vary across species. In *Aspergillus fumigatus*, the etiological agent of invasive aspergillosis, septins participate in a variety of processes such as cell wall organization of conidia, septation, and response to cell wall stress. Previous studies determined that the Δ*aspB* strain had a greater sensitivity to anti-cell wall drugs, especially the echinocandin caspofungin, yet mechanisms behind this augmented sensitivity are unknown. We performed cell viability staining of the deletion strains post-caspofungin exposure and found that the Δ*aspA*, Δ*aspB*, and Δ*aspC* strains have significantly lower cell viability. Concomitant with the reduced viability, deletion strains are more susceptible to caspofungin on solid media. These results indicate that the septin cytoskeleton is important for *A. fumigatus* survival in the presence of caspofungin. Due to the potential of improved therapeutic outcome, we followed up using a neutropenic murine model of invasive aspergillosis. Animals infected with the Δ*aspB* strain and treated with caspofungin showed improved survival compared to the animals infected with *akuB*^{KU80} wild-type or complemented strains. Additionally, histological analysis showed reduced fungal burden and inflammation in the Δ*aspB* infected, caspofungin-treated group. Affinity purification coupled with quantitative proteomics identified proteins involved in the septin-dependent response to caspofungin, includng four candidate interactors involved in cell wall stress response. Deletion of these candidate genes resulted in increased susceptibility to caspofungin and moderately reduced viability post-drug exposure. Taken together, these data suggest that septin AspB contributes to the fungistatic response to caspofungin.

Author Summary:

Invasive aspergillosis is a pulmonary disease caused by the fungus *Aspergillus fumigatus* that primarily occurs in immunocompromised patients. Invasive aspergillosis has a high mortality rate, ranging from 50-90%. Therapy options are limited due to few available drugs with fungicidal activity and growing global drug resistance. Treatment typically starts with triazoles, which target the fungal cell membrane. If unsuccessful, an echinocandin, which targets the cell wall, is given as a salvage therapy. Echinocandins, including caspofungin, are fungistatic against *A. fumigatus*, slowing growth of the fungus rather than killing it. Due to this, echinocandins have a high therapeutic failure rate. Previous work suggests that deletion of the cytoskeletal septin genes increases sensitivity to caspofungin. Here we describe our finding that the septin genes *aspA, aspB*, and *aspC* are involved in the fungal response to caspofungin. Additionally, the deletion of *aspB* results in fungicidal activity of this otherwise fungistatic drug. These findings show promise for novel therapy options that block the septin-mediated response to caspofungin.

Introduction:

Aspergillus fumigatus is a ubiquitous environmental mold responsible for a wide range of opportunistic systemic and allergic pathologies [1]. One such pathology is invasive aspergillosis (IA), an invasive systemic infection most common in immunocompromised patients [2]. Over 300,000 cases of IA are reported yearly, leading to a mortality rate ranging between 30-90% [1,3]. The at-risk patient population for IA is increasing due to increasing numbers of immunomodulating therapies, as well as emerging global diseases [4–6]. Additionally, IA has the highest per-patient cost of any invasive fungal disease, costing the United States an estimated $1.3 billion per year [7].

IA begins when the conidia, or asexual spores, are inhaled by an individual. The conidia are easily aerosolized and are prevalent in both indoor and outdoor environments [8,9]. Due to their small size (~2.5 µm diameter) and hydrophobic nature, the conidia can travel down the airway into the terminal alveoli [10]. In healthy individuals, the mucociliary escalator removes conidia [8]. However, any remaining conidia can then germinate within the lung. Epithelial cells, alveolar macrophages, neutrophils, and other immune cells can detect the germinating conidia, which leads to the release of cytokines and phagocytosis of conidia by immune cells [8]. In immunocompromised patients, the lack of immune responses leads to the progression of IA. Germinated conidia can then establish polarity, leading to the formation of hyphae that invades host tissue. IA can disseminate within the host via the release of hyphal fragments into the bloodstream. Neutropenic patients, such as those on anti-rejection medications post-transplant, are at high risk for IA [11]. In neutropenic patients, disease often presents with abundant hyphal growths, angioinvasion, and intra-alveolar hemorrhage [12,13]. Patients undergoing corticosteroid-induced immunosuppression are also at risk of IA, as glucocorticoids lead to a reduction of pattern recognition receptor (PRR) signaling and inhibit lymphocyte activation [14,15]. Pneumonia, inflammatory necrosis, and minimal hyphal growths are seen in cases of IA in patients under corticosteroid-induced immunosuppression [12,13]. Therapeutic options to effectively treat IA are limited. The frontline treatment for IA is the triazole class of drugs [16]. Triazole treatments are often prolonged and are now common to use as antifungal prophylaxis in at-risk populations. Nonetheless, cases of triazole-resistant *A. fumigatus* infections are becoming more common. This increase in the incidence of azole resistance led to the inclusion of *A. fumigatus* as a critical priority in the World Health Organization 2022 Fungal Priority Pathogens List [17].

Echinocandins are a class of antifungals that target the cell wall via β-glucan synthase [18]. In fungi such as *C. albicans*, echinocandins have a fungicidal effect [19]. In contrast, the echinocandins are fungistatic against *A. fumigatus* [18]. For immunocompromised patients, the echinocandins are often used as a salvage or secondary therapy in conjunction with triazoles as they cannot reap the benefits of solely fungistatic medications [16]. Slowing the growth of the fungi through fungistatic therapies then requires either the immune system or fungicidal drugs to kill the fungi and clear disease [20,21]. Because of its fungistatic nature, caspofungin use as a salvage treatment had a favorable response rate of only 45% [22]. Understanding the mechanisms within fungi that render these medications fungistatic rather than fungicidal can aid in developing new therapies that improve the efficacy of existing antifungal drugs.

Previous studies have shown that septins AspA, AspB, and AspC contribute to the *Aspergillus* spp. response to the echinocandin caspofungin [23,24]. Septins are a family of highly conserved eukaryotic GTP-binding proteins. In *A. fumigatus,* septins are primarily involved in septation, conidiation, and response to cell wall stress [24]. *A. fumigatus* has five septins: AspA, AspB, AspC, AspD, and AspE [25]. AspA-D are core mitotic septins involved in polymerizing into hexameric and octameric complexes. They are orthologs of *Saccharomyces cerevisiae*'s Cdc11, Cdc3, Cdc12, and Cdc10, respectively [26]. AspE is a group 5 septin that is present in filamentous fungi and other eukaryotic lineages [27]. Septins also can scaffold proteins involved in stress response pathways. *Candida albicans* septins and phospholipid $PI(4,5)P_2$ are regulated in response to cell wall stress induced from caspofungin exposure [28]. They relocalize at specific foci on the plasma membrane to activate the MAPK Mkc1, which then relocalizes chitin synthase and results in chitin deposition in the cell wall [28–30]. Similarly, *Aspergillus nidulans* septins have been associated with the cell wall integrity (CWI) pathway [23]. Double deletion strains of *aspB* and CWI pathway MAPK *mpkA* showed a novel phenotype

when grown on caspofungin compared to the respective single deletion strains [23]. These data suggest AspB may have a role in pathways that maintain CWI.

In this study, we found that septins AspA, AspB, and AspC contribute to fungal viability post-caspofungin exposure in *A. fumigatus*. The deletion of *aspB* in particular produced a fungicidal response. We also observed a higher chance of survival, reduced lung inflammation, and reduced fungal burden was associated with Δ*aspB* infected mice treated with caspofungin than Δ*aspB* strain treated with saline or *akuB*^{KU80} and Δ*aspB::aspB* strains with either treatment in our neutropenic murine model of IA. To gain deeper mechanistic insights, we conducted a quantitative mass spectrometry-based proteomics analysis to identify candidate AspB-interacting proteins during exposure to caspofungin. Based on our proteomics analysis, we narrowed down six possible proteins involved in the fungal response to caspofungin that were significantly increased (by at least two-fold) upon caspofungin exposure. Gene ontology (GO) analysis indicated that these candidate protein interactors might have a role in cell wall function and organization, suggesting that AspB may mediate cell wall responses through its interactions with these candidates. Deletion strains for each candidate were generated and characterized to obtain an understanding of their biology at basal conditions. Strains were then tested against caspofungin, and four out of the six genes, *bgt1, gel2, nsdD*, and *mapA*, were implicated in fungal viability after caspofungin exposure.

Results:

Deletion of aspA*,* aspB*, and aspC Reduces Viability Post-Caspofungin Exposure*

Previous work demonstrated the hypersensitivity of *A. fumigatus* Δ*aspB* strain and sensitivity of Δ*aspC* strain to caspofungin on solid media [24]. In order to further confirm and characterize the

response of septins to echinocandins, we conducted a spore dilution assay (10^4-10^1 conidia, 1 µg/mL caspofungin), minimum effective concentration assay (MEC), and E-strip test (10^6 conidia) to visualize the susceptibility to caspofungin. Deletion of the core septin genes, *aspA, aspB*, and *aspC*, resulted in increased sensitivity to caspofungin compared to the *akuB*^{KU80} wild-type strain, Δ*aspB::aspB* complemented strain, and other septin deletion strains (Fig. 1A, Supplementary Table 4). Similarly, the Δ*aspA*, Δ*aspB*, and Δ*aspC* strains had a clearer and larger zone of effect on the E-strip test (Fig. 1D). To explore whether this effect was exclusive to caspofungin, we conducted an E-strip test to visualize the susceptibility to another drug in the echinocandin class, micafungin. The Δ*aspA and* Δ*aspC* strains showed a slight increase in sensitivity to micafungin, while Δ*aspB* had a more noticeable decrease in growth in the zone of effect (Fig. 1D). Thus, this increase in susceptibility of the Δ*aspA,* Δ*aspB*, and Δ*aspC* strains is not limited to caspofungin, albeit it is more pronounced.

AspB is Required for Fungistatic Response to Caspofungin in vitro

Since we observed an increase in susceptibility in all three of our drug susceptibility assays, we hypothesized that the absence of AspA, AspB, and AspC leads to a fungicidal effect of caspofungin. To determine viability of the deletion strains against caspofungin, we utilized CFDA to determine cell viability post-caspofungin exposure. In basal conditions, 10^4 conidia were grown on coverslips in GMM liquid media for 24 hours, followed by 1 hour incubation in 1 µg/mL CFDA. All strains are equally viable, indicating that the increased clearance is not due to a reduction in viability of septin deletion strains (Fig. 2A). Strains were then grown for 48 hours in the presence of 1 µg/mL caspofungin, followed by incubation with CFDA. The *aspA, aspB*, and *aspC* deletion strains were significantly less viable ($p<0.0001$) after 48 hours of caspofungin exposure, with only 0.92% of Δ*aspB* ($p<0.0001$) being viable (Fig. 1B, 2B). Δ*aspB* also does not form many microcolonies in the presence of caspofungin. Δ*aspA* and Δ*aspC* form microcolonies

in the presence of caspofungin; however, only 16.3% and 18.5% of the colonies, respectively, were viable at the time of microscopic examination ($p<0.0001$)(Fig. 1B, 2B). We repeated this assay with the echinocandin micafungin in order to test if this reduction in viability was specific to caspofungin or a general response to echinocandin exposure. In contrast to caspofungin treatment, the majority of colonies from all strains were viable after micafungin treatment (Fig. 1C). This indicates that the reduction in viability is specific to caspofungin.

AspB is Involved in Response to Caspofungin in Mature Mycelium

It is possible that most of these phenotypes that we observe are due to caspofungin acting as the mycelia germinates, as exemplified by the small microcolonies in the Δ*aspB* strain. Mature mycelia would be a more clinically relevant growth stage, and for this reason, we decided to determine the effect of caspofungin on mature mycelium. To test this, we used propidium iodide (PI) stain to determine hyphal damage. Strains were grown in GMM+UU for 24 hours at 37°C before being stained with PI solution and visualized. No hyphal damage was seen under basal conditions (Fig. 3A). Following the same procedure, we grew strains then incubated them with caspofungin (1 µg/ml) for 2 hours. Plates were washed and stained as before, then visualized. Similar to our viability assays, only the Δ*aspB* strain exhibits extensive hyphal damage after 2 hours of exposure to caspofungin (Fig. 3B). Taken together, these results suggest that AspB is needed for fungal response to caspofungin.

Deletion of aspB *improves caspofungin treatment efficiency in a neutropenic murine model of invasive aspergillosis*

As we observed a strong fungicidal effect against the Δ*aspB,* we decided to determine if deletion of *aspB* led to improved survival in our murine model of invasive aspergillosis. As the

191 Δ*aspB* strain has no discernable difference in virulence compared to the *akuB*^{KU80} and
192 Δ*aspB::aspB* strains with respect to fungal burden and lung inflammation, any effect on survival
193 would be attributed to the role that AspB plays in fungal response to caspofungin [24]. To test
194 this hypothesis, neutropenia was induced in 6-week old male CD-1 mice using 175 mg/kg
195 cyclophosphamide and 40 mg/kg triamcinolone acetonide. Neutropenic mice were then
196 intranasally infected with 4×10^6 conidia of *akuB*^{KU80}, Δ*aspB*, and Δ*aspB::aspB* strains. They
197 were subsequently treated with either 2 mg/kg caspofungin or an equivalent volume of the
198 saline vehicle. All groups of mice treated with saline all had the first death on day 3 post-
199 infection (Fig. 4A). Mice inoculated with Δ*aspB* strain and treated with caspofungin had a 70%
200 probability of survival ($p<0.0001$)(Fig. 4B). Additionally, in this group the first death did not occur
201 until day 12 post-infection. Compared with the next highest groups, ∆*aspB* strain treated with
202 saline and *akuB*^{KU80} treated with caspofungin had a 30% probability of survival (Fig. 4A). Lung
203 histology was then performed to visualize inflammation and fungal lesions. Concurrent with the
204 survival graph, animals infected with the Δ*aspB* strain treated with caspofungin had reduced
205 inflammation and stunted fungal growth compared to animals from the other groups (Fig. 4D).
206 Previous infection models also showed no difference in inflammation or fungal lesions between
207 untreated *akuB*^{KU80}, Δ*aspB*, and Δ*aspB::aspB* strains [24]. This suggests the caspofungin
208 treatment reduces growth or potentially has a fungicidal effect on the fungus without AspB *in*
209 *vivo*, as well.

210

211 *AspB Interactome Changes Post Caspofungin Exposure*

212 Previous work determined that septins' localization is altered by exposure to caspofungin in *C.*
213 *albicans* and *A. fumigatus* [24,28]. Additionally, the protein interactome of septin AspB was
214 altered after exposure to caspofungin in a qualitative proteomic experiment [31]. This work only
215 detected for the presence or absence of interactant proteins between basal and caspofungin

conditions, potentially missing interactions that occur in both conditions but change in abundance [31]. To gain a more mechanistic insight into how AspB contributes to the fungal response to caspofungin, we applied affinity purification coupled with quantitative proteomics. An AspB-eGFP expressing strain was grown in GMM and GMM supplemented with 1 µg/mL caspofungin for 24 hours. AspB-GFP was then purified using a GFP-Trap® affinity matrix, and proteins bound to AspB-GFP were prepared and analyzed by LC-MS/MS to identify protein interactors in each condition. Principal Component Analysis (PCA) indicates that the GMM- and caspofungin-AspB interactome are distinctive from each other (Fig. S1A). A total of 226 proteins were significantly decreased (fold change (FC) < -2, $p < 0.05$) and 106 proteins were significantly increased (FC > 2, $p < 0.05$) upon caspofungin treatment (Fig. S1B). Among the proteins increased upon caspofungin exposure was PpoA, a characterized fatty acid monooxygenase. PpoA was also identified by a previous study investigating the AspB interactome post-caspofungin exposure, indicating that our analyses were able to confirm previously described caspofungin-specific AspB interactions [31]. Candidate protein interactors that met the screening criteria were analyzed using FungiFun, a gene ontology tool, to assess changes in biological processes [32]. Proteins that are known to be involved in hyphal growth were overrepresented among the list of proteins increased upon caspofungin treatment (Fig. S1C). In contrast, proteins that are known to be involved in protein folding were overrepresented in the list of proteins decreased upon caspofungin treatment (Fig. S1D). Using this information, we selected six genes that were significantly increased by at least two-fold (FC > 2, $p < 0.05$) after caspofungin exposure and had a role or putative role in cell-wall related functions for further investigation (Table S3).

241 Δbgt1, Δgel2, ΔnsdD*, and* ΔmapA *Have a Reduction in Conidiation, While* ΔnsdD *and* ΔpunA
242 *Have a Growth Defect*

243 Based on our proteomics and gene ontology analyses, we performed the deletion of all six
244 candidate genes (Table S3) to determine their role in septin-related phenotypes. We first
245 characterized each deletion strain to understand how the gene affects growth during basal
246 conditions. Major and biologically relevant radial growth defects are seen in Δ*nsdD* (37.8 mm
247 average diameter compared to the 85 mm diameter of the *akuB*^{KU80} strain) and Δ*punA* (24.3 mm
248 average diameter compared to the 57.3 mm average diameter of the *akuB*^{KU80} strain at
249 30°C)(Fig. 5A, 5D, Fig.S2). The slight reduction of radial growth in Δ*aspB* was also seen in a
250 previous study and deemed not biologically relevant, which is also the case for the Δ*gel2* strain
251 [24]. Similarly, a previously noted defect in conidiation was seen in Δ*aspB* [24]. Δ*bgt1,* Δ*gel2,*
252 Δ*nsdD*, and Δ*mapA* also have reduced conidiation, but not as severely as Δ*aspB* (Fig. 5B, 5E).
253 As prior work noted that Δ*aspB* strain had delayed septation, we were interested in determining
254 if any of the candidate gene deletion strains were also defective in septation [24]. To test this,
255 we measured apical compartment length as an indirect method of measuring potential septation
256 defects. Δ*bgt1* mutants have a similar increase in apical compartment length to Δ*aspB*,
257 suggesting a delay in septation (Fig. 5C). In contrast, Δ*gel1* mutants have apical compartments
258 similar to the *akuB*^{KU80} wild-type strain (Fig. 5C), suggesting that Gel1 is dispensable for septa
259 formation. Δ*gel2* (70.4 µm) and Δ*mapA* (67.7 µm) mutants exhibit hyperseptation. Δ*nsdD* (37.7
260 µm) has a more drastic reduction in apical compartment length, but this phenotype may be due
261 to its growth defect (Fig. 5C).

262

263

264

Δbgt1, Δgel2, ΔnsdD*, and* ΔmapA *Have Increased Sensitivity to Caspofungin Exposure*

Since the candidate proteins showed increased interaction with AspB during caspofungin exposure, we explored their potential role in mediating the AspB-dependent fungal response to caspofungin. To test this, we conducted a spore dilution assay on GMM agar supplemented with 1 µg/mL caspofungin. 10^4, 10^3, 10^2, and 10^1 spores were plated and incubated at either 30°C or 37°C for 2 days. Deletion of the *aspB* gene displayed colony-level growth defects in the 10^3, 10^2, and 10^1 concentrations (Fig. 6A, 6C). No other deletion strains displayed as severe of a sensitivity to caspofungin. Δ*bgt1,* Δ*gel2,* Δ*nsdD*, and Δ*mapA* lost full colony growth at 10^2 and 10^1 concentrations (Fig. 6A). In contrast, Δ*gel1* and Δ*punA* are similar to the *akuB*^{KU80} wild-type and Δ*aspB::aspB* complemented strains (Fig. 6A, 6C). The minimum effective concentration (MEC) of caspofungin for Δ*bgt1,* Δ*gel2,* Δ*nsdD*, and Δ*mapA* was determined to be lower than that of the wild-type, and equal to or lower than that of Δ*aspB* (Table S4). Δ*punA* was not determined as CLSI standards require 37°C, and this strain cannot grow at that temperature.

Reduced Viability of Δbgt1, Δgel2, ΔnsdD*, and* ΔmapA *Post-Caspofungin Exposure*

Since *aspB* deletion leads to a fungicidal response to caspofungin, we investigated whether any candidate gene deletion strains also exhibited reduced viability. All strains showed equal viability in basal conditions (Fig. 7A, 7C). We then grew all strains for 48 hours in the presence of 1 µg/mL caspofungin and determined their viability with CFDA. The *aspB* deletion strain showed nearly no viability at both 30°C and 37°C, as previously shown in Figure 1B (Fig. 6B, 6D and Fig. 7B, 7D). No other strain demonstrated the complete loss of viability phenotype observed in the Δ*aspB*. The Δ*bgt1*, Δ*gel2*, Δ*nsdD*, and Δ*mapA* strains form microcolonies in the presence of caspofungin like the *akuB*^{KU80} strain, but they had a reduction in viability (Δ*bgt1*=37.4%, Δ*gel2*=39.5%, Δ*nsdD*=27.8%, Δ*mapA*=26.1% compared to *akuB*^{KU80}

289 =90.4%)(Fig 6B and Fig.7B). Δ*gel1* and Δ*punA* did not have a reduction in cell viability when
290 grown in caspofungin (Fig. 6B, 6D and Fig. 7B, 7D).

291

292 *Bgt1, Gel2, NsdD, and MapA are Involved in the Response to Caspofungin in Mature Mycelium*

293 Next, we determined if any of our candidate gene deletion strains were susceptible to hyphal
294 damage when exposed to caspofungin as mature mycelia. To visualize hyphal damage, we
295 utilized a propidium iodide (PI) stain. No hyphal damage was observed in basal conditions,
296 indicating that there is no defect in the cell wall at basal conditions (Fig. 8A, 8C). The
297 experiment was then repeated with a 2-hour incubation in GMM supplemented with 1 µg/mL
298 caspofungin prior to PI staining. Extensive hyphal damage was seen in Δ*bgt1*, Δ*gel2*, Δ*nsdD*,
299 and Δ*mapA* strains similar to Δ*aspB* after exposure to caspofungin (Fig. 8B). Taken together,
300 Bgt1, Gel2, NsdD, and MapA are involved in the fungal response to caspofungin in earlier
301 stages of growth and mature hyphae.

302

303 *Candidate Genes are not involved in the response to other Cell Wall Disrupting Agents or in the*
304 *Caspofungin Paradoxical Effect*

305 We further characterized the candidate gene deletion strains sensitivities to other cell wall
306 disturbing agents. To test this, we plated conidia on GMM agar and GMM supplemented with
307 either 1 µg/mL caspofungin, 100 µg/mL Congo red, 2 µg/mL nikkomycin Z, 5 µg/mL calcofluor
308 white, or 10 µg/mL calcofluor white and incubated for three days. Additionally, we plated 4
309 µg/mL caspofungin and incubated for five days to observe whether the deletion strains were still
310 capable of the caspofungin paradoxical effect. After incubation, Δ*aspB* shows increased
311 susceptibility to caspofungin and Congo red, and slight increase in susceptibility to nikkomycin Z
312 and calcofluor white (Fig. S3). We observed *Δgel1* had a mild increase in susceptibility to Congo

313 red compared to the *akuB*^{KU80} wild-type (Fig. S3). Δ*bgt1*, Δ*gel2*, and Δ*nsdD* had a mild increase
314 in susceptibility to 10 µg/mL calcofluor white, but not as pronounced as Δ*aspB* (Fig. S3). Δ*punA*
315 visually appeared to have a reduction in conidiation and abnormal colony morphology when
316 grown on nikkomycin Z, but no differences in growth when compared to the wild type strain (Fig.
317 S4). Taken together, these candidate genes might mediate fungal response to caspofungin
318 while not being a part of a general fungal cell wall stress response.

319

320 **Discussion:**

321 The septins are a highly conserved family of cytoskeletal proteins with a variety of cellular roles.
322 This includes roles in cell division, stress response, cytoskeleton organization, and scaffolding
323 [24,33–35]. Previous work noted the role of septins in response to cell wall stress. In *C.*
324 *albicans*, septins are required for proper cell wall regulation and mislocalize during exposure to
325 caspofungin [29,36]. Additionally, septins also mislocalized during basal conditions in deletion
326 strains of protein kinases involved in cell wall regulation, including Gin4, Kin3, Vps34, and Cbk1
327 [36]. In *A. nidulans*, *C. albicans*, and *S. cerevisiae*, chitin synthases are dependent on septins
328 for proper localization [29,37,38]. Previous work in *A. fumigatus* determined that the septins
329 have a role in response to cell wall stress, notably showing that Δ*aspB* exhibits a hypersensitive
330 response to caspofungin exposure on solid media [24]. Here, we aimed to further investigate the
331 septin response to caspofungin. We found that deletion of *aspA, aspB*, and *aspC* showed a
332 reduction in fungal viability post-caspofungin exposure, while deletion of *aspB* elicited a
333 fungicidal response. The deletion of *aspB* also increased hyphal damage in mature mycelia.
334 The Δ*aspB* response to caspofungin was also recapitulated in an *in vivo* murine model, with
335 Δ*aspB* infected mice showing higher survival rates, reduced inflammation, and delayed mortality
336 upon treatment with caspofungin.

337

The *Aspergillus spp.* septins form heteropolymers consisting of hexamers (AspA-C) and octamers (AspA-D) [39]. Deletion of *aspD* still allows proper formation of hexamers but not octamers. In our work, we found that *aspA, aspB*, and *aspC* deletion strains had reduced viability to caspofungin (Fig. 1). While the *aspD* deletion strain was slightly more sensitive than the *akuB*^{KU80} wild-type, Δ*aspB::aspB*, or Δ*aspE* strains, its increased susceptibility was not as pronounced as that of the *aspA*, *aspB*, and *aspC* deletion strains. This suggests that the presence of the hexamer is at least sufficient, if not necessary, for proper fungal response to caspofungin. It is unknown if only the sole presence of the octamer would also be sufficient, as deletion of *aspA-C* prevents the formation of both structures. Similarly, Δ*aspB* strain had a hypersensitive to fungicidal response to clinically relevant doses of caspofungin (Fig. 1), more drastic than the one observed in the Δ*aspA* or Δ*aspC* strains. It is possible that AspB specifically is needed to scaffold necessary proteins in response to caspofungin, but the loss of both the hexamer and octamer causes general dysfunction that would lead to the phenotypes seen in Δ*aspA* or Δ*aspC*. Proteomics analysis in *Cryptococcus neoformans* also supports the possibility of subunit-specific protein interactions, where the *cdc3*^{aspB} and *cdc10*^{aspD} septins are shown to have differences in interactomes after exposure to cellular stressors [40]. All of the septin deletion strains retain the caspofungin paradoxical effect, suggesting that individual septins and their heteropolymers act independently of the pathways that contribute to the caspofungin paradoxical effect.

We found that the septin response to echinocandins is not limited to caspofungin, but the fungicidal response of Δ*aspB* is specific to caspofungin. The echinocandin class includes four clinically approved drugs: anidulafungin, micafungin, caspofungin, and most recently approved,

rezafungin [41,42]. These drugs all work through noncompetitive inhibition of the β-1,3-D-glucan synthase, but alterations in their side chains comprise the major differences between each one [18,43]. These changes in the side chains can lead to changes in how the drug impacts fungal physiology. For instance, caspofungin is the only echinocandin to induce the paradoxical effect [43]. Unlike micafungin, high concentrations of caspofungin increase the levels of cytosolic calcium [44,45]. This activates calmodulin-calcineurin signaling and leads to the caspofungin paradoxical effect [45]. Thus, our findings add to the growing evidence that even though the different echinocandins have a shared mechanism of action, how the fungus responds to echinocandins is drug specific.

Hyphal damage was not observed in any of our strains, indicating that there is no underlying cell wall defect that would cause damage in basal conditions. However, after 2-hour exposure to caspofungin, the Δ*aspB* strain showed significant hyphal damage. This suggests that AspB is involved in the fungal cell wall response to caspofungin in mature mycelium. In *C. albicans*, caspofungin has a fungicidal effect. Phosphatidylinositol-(4,5)-bisphosphate and septin regulation are needed for proper cell wall stress response [28]. Disruption of either party causes hypersusceptibility to caspofungin [28,29]. Based on our analyses, AspB is needed for proper cell wall response to caspofungin in *A. fumigatus*. Previous proteomic analyses and our own proteomics experiments show that MpkA, MkkA, and other cell wall integrity kinases co-immunoprecipitated with AspB [31]. It is possible that AspB interacts with the cell wall integrity pathway in *A. fumigatus* to facilitate fungal response to caspofungin [31]. In *A. nidulans,* deletion of *aspB* partially rescues both the growth defect and susceptibility to caspofungin of the Δ*mpkA* strain, further hinting a possible crosstalk between the septin and the CWI [23]. Further work will be needed to investigate the possible role of AspB in the cell wall integrity pathway.

386 Animals infected with the Δ*aspB* strain and treated with caspofungin had a 70% chance of
387 survival, which is higher than that of animals infected with *akuB*^{KU80} strain (30%). The first death
388 of ∆*aspB* strain infected mice treated with caspofungin was recorded on day +12 post infection,
389 compared to Δ*aspB* strain infected mice treated with saline or the other strains and conditions
390 with first deaths on day +3 or day +4. It is possible that colonies that persist under caspofungin
391 treatment are capable of growing and establishing infection after the drug pressure is released.
392 Our histological analyses showed reduced inflammation and reduced fungal lesions in the lungs
393 of Δ*aspB* infected mice treated with caspofungin. However, this assay is done on day +3 after
394 infection when mice are still being treated with caspofungin. Nonetheless, this increase in
395 survival makes AspB a prospective target for drug therapy developments, as use in conjunction
396 with caspofungin elicits a fungicidal response in *A. fumigatus*. Currently, only the plant cytokinin
397 forchlorfenuron (FCF) is known to disrupt septin organization [46]. This compound disrupts
398 septins within both fungal and mammalian cells by interfering with their ability to bind and
399 hydrolyze GTP [46–48]. It is possible that FCF could be modified and refined to target fungal-
400 specific septins. FCF analogues have previously been developed to better target ovarian and
401 endometrial cancers [49]. Thus, FCF analogues could be used in conjunction with caspofungin
402 to create a new fungicidal therapy for treatment of IA. Further work is required to better
403 understand the mechanisms of AspB's response to caspofungin and to develop novel clinical
404 therapies.

405

406 Our proteomic analysis uncovered six candidate protein interactors of septin AspB that were
407 significantly increased upon caspofungin treatment and that have a potential role in cell wall
408 functions. Bgt1, Gel1, and Gel2 are glucanosyltransferases in *A. fumigatus* [50]. These
409 glucanosyltransferases work to remodel unorganized β-1,3-glucan chains in the periplasmic
410 space to stabilize and modify the cell wall as needed [50]. Due to their role in cell wall

411 homeostasis, previous work identified these three glucanosyltransferases as potential drug
412 targets that required further investigation [50]. Bgt1 works by hydrolyzing a β-1,3-linked
413 oligosaccharide and placing it on another molecule of β-1,3-glucan [51]. In *C. albicans*, deletion
414 of *BGL2*, the *bgt1* homologue, resulted in an increase in susceptibility to nikkomycin Z, a chitin
415 synthase inhibitor [52]. In contrast, *A. fumigatus* Δ*bgt1* only has a slight increase in susceptibility
416 to nikkomycin Z (Fig. S3). Deletion of *BGL2* in *S. cerevisiae* increased the cellular chitin content
417 [53]. In *A. fumigatus,* though, Δ*bgt1*Δ*bgt2* double mutants do not have a change in chitin content
418 [51]. A slight reduction in conidiation was observed in *A. fumigatus* Δ*bgt1* (Fig. 5A, 5B). *A.*
419 *fumigatus* Δ*bgt1* susceptibility to calcofluor white and Congo red were similar to the *akuB*^{KU80}
420 wild-type, although compared to basal conditions there was a reduction in growth (Fig. S3) [54].
421 A potential mechanism for the increased susceptibility in *A. fumigatus* Δ*bgt1* and Δ*aspB* to
422 caspofungin is that hyphal damage may be exacerbated by the lack of interaction between
423 AspB and Bgt1 when either party is missing (Fig. 6B). Due to the role of septins in septation and
424 scaffolding, the loss of AspB in particular may be more deleterious than just the loss of Bgt1 and
425 thus result in the observed fungicidal effect (Fig. 1B). Further work is needed to uncover the
426 relationship between glucanosyltransferase Bgt1 and the septins in septation and cell wall
427 stress responses.

428

429 Gel1 and Gel2 are two GPI-anchored glucanosyltransferase members of the Glycoside
430 Hydrolase Family 72 (GH72) [55]. Despite having the same enzymatic activity, deletion of *gel1*
431 did not result in a unique phenotype, but reduced mycelial growth and abnormal cell wall
432 architecture was observed in Δ*gel2* during basal conditions (Fig. 5A-B) [50,51,56]. An increase
433 in chitin is associated with deletion of *gel2*, a compensatory mechanism similar to deletion of
434 *bgt1* [56]. *A. fumigatus* Gel1 is dispensable for proper fungal response to caspofungin (Fig. 6 A-
435 B). In contrast, Gel2 does appear to be involved in the response to caspofungin due to

increased susceptibility to caspofungin and reduced viability in caspofungin compared to *akuB*^{KU80} wild-type (Fig. 6A-B). Our proteomics analysis noted an increased interaction between Gel2 and AspB, but cellular levels of Gel2 were not explored. It is unknown if cellular levels of Gel2 are increased in *A. fumigatus* post-caspofungin exposure similar to *C. albicans*. Additionally, further work exploring overexpression of Gel2 may uncover a new mechanism of resistance to caspofungin in *A. fumigatus*.

NsdD (**n**ever in **s**exual **d**evelopment) is a putative GATA-type transcriptional activator with roles in *A. nidulans* for sexual development [57]. NsdD is responsible for activating sexual development [58]. Deletion of *nsdD* results in the inability to produce cleistothecia (fruiting bodies), while overexpression allows production of Hülle cells even in conditions which typically block sexual development [58]. Despite being a primarily asexual fungus, *A. fumigatus* is capable of and still holds a variety of functional sexual reproductive genes [59]. NsdD has been implicated in cell wall remodeling and hyphal fusion [60]. Deletion of *nsdD* results in reduced hyphal growth on minimal media (Fig. 5B) [57,60]. Additionally, mating done with Δ*nsdD* resulted in impaired heterokaryon formation [60]. Drug challenges show some sensitivity of Δ*nsdD* to Congo red and caspofungin (Fig. 6A-B, Fig. S3) [60]. Previous work also noted weakened hyphal tips in Δ*nsdD*, which is in accordance with the increased hyphal damage during cell wall stress seen via PI staining (Fig. 8B) [60]. We suspect that while NsdD may have independent roles in sexual development, it is possible that previous cell wall remodeling functions of NsdD seen during hyphal fusion for heterokaryon formation may have alternative functions in *A. fumigatus* cell wall remodeling outside of sexual development. Further work is required to understand the NsdD-mediated response to caspofungin exposure.

MapA (gene *Afu4g06930*) is a previously uncharacterized protein in *A. fumigatus*. In *S. cerevisiae* and *C. albicans*, cytosolic protein MAP2 is an ortholog that functions as a methionine aminopeptidase. Deletion of MAP2 results in slightly slower growth rate and some chemical sensitivities in *S. cerevisiae* and *C. albicans* [61,62]. It is possible that this methionine aminopeptidase can remove the methionine to promote maturation of protein involved in response to caspofungin.

PunA (gene *Afu6g07470*) is a previously uncharacterized protein in *A. fumigatus*. In yeast, *PUN1* is a Sur7 family tetraspan that localizes in eisosomes/MCC (membrane compartment of Can1) [63,64]. These punctate membrane domains have roles in stable furrowing and promote stress resistance, including detecting and responding to changes in cell wall integrity [63]. Deletion of *PUN1* resulted in decreased thermotolerance, abolished filamentous growth, reduced cell wall components, and decreased metal ion tolerance [65–67]. This decreased thermotolerance was also observed in our *A. fumigatus* Δ*punA* strain, thus requiring the growth of Δ*punA* and comparison strains at 30°C. Yeast deletion strains of *SUR7*, a closely related protein, saw little sensitivity to caspofungin but high sensitivity to the triazole fluconazole [68]. Interestingly, a previous study in *A. fumigatus* noted an increase in gene expression of *punA* post-exposure to the triazole voriconazole [69]. *A. fumigatus* Δ*punA* had a similar phenotype to the *akuB*^{KU80} wild-type when exposed to caspofungin or other cell wall stressors (Fig 6C-D, Fig. S4). It is possible that *A. fumigatus* PunA contributes to the fungal response to non-cell wall stressors, such as metal ion stress or membrane targeting drugs. It is also possible that PunA might contribute with septin localization post-caspofungin exposure; however, this possible role in septin localization does not contribute to *A. fumigatus* susceptibility to caspofungin.

There is increasing evidence that the septins are involved in the mediation of cell wall stress [23,24,28,29,31]. In this work, we demonstrate that the septin hexamer is sufficient for response to caspofungin and the deletion of the septin gene *aspB* results in a fungicidal effect. This phenotype continues *in vivo*, suggesting potential therapeutic applications. We also identified four AspB interactors that are involved, but not required, in the fungal response to caspofungin. Overall, we suggest that the deletion of *aspB*, and thus loss of all AspB's interactions, results in the fungicidal effect of caspofungin demonstrated. Future studies directed towards developing drugs specific to fungal septins or in determining additional septin interactants that have key roles in the caspofungin response can help to better understand ways in which caspofugnin therapy can be improved for use against invasive aspergillosis.

Materials and Methods:

Strains, media, and conditions:

A. fumigatus akuB^{KU80} served as the wild-type and control strain. Δ*aspB::aspB* complemented strain served as an additional control to determine that phenotypes were due to the deletion of the *aspB* gene. Septin deletion strains are described in (Table S1, [24,70]). The *aspB-egfp* strain from [24], with *aspB-egfp* expressed by the *aspB* promoter from the native loci, was used to pulldown AspB interactants. All cultures were plated on glucose minimal media (GMM) supplemented with 5 mM uracil and 5 mM uridine (GMM+UU) and incubated at 37°C, unless otherwise specified.

Drug susceptibility assays:

Spores were counted, diluted, and inoculated in rows onto agar plates containing caspofungin (1 µg/mL) in 10µL quantities with a total of 10^4, 10^3, 10^2, and 10^1 conidia. Plates were incubated for 48 hours at 37°C unless otherwise noted. For the minimum effective concentration assay, a quantity of $2.5x10^4$ spores were added to RMPI media with different concentrations of caspofungin and incubated for 48 hours at 37°C [71]. We were not able to test the *aspD* and *punA* deletion strains according to CLSI guidelines as Δ*aspD*, which is an uracil/uridine auxotroph, could not grow in RMPI, and Δ*punA*, which has a temperature sensitivity, could not grow at 37°C.

Fungal Viability Assay:

Conidia of *akuB*^{KU80}, Δ*aspA-E*, and Δ*aspB::aspB* were diluted to 10^4 spores and cultured on coverslips immersed in 4 mL of GMM+UU broth and GMM+UU+caspofungin (1 µg/ml) and incubated at 37°C for 24 and 48 hours, respectively. To examine cell viability, coverslips were incubated in 5-carboxyfluorescein diacetate (CFDA) (50 µg/mL 0.1 M MOPS pH 3) for 1 hour at 37°C and 70 rpm. Slides were prepared for microscopy and image on an Inverted Leica DMi8 with Leica K5 Microscope Camera using a 10x objective. Images were analyzed using imageJ [72]. Viable colonies were quantified by counting colonies manually and dividing fluorescent colonies over total colonies counted. A minimum of 50 colonies per strain per replicate were counted.

Hyphal damage assay:

Conidia (10^4) of *akuB*^{KU80}, Δ*aspA-E*, and Δ*aspB::aspB* were cultured on coverslips immersed in 4 mL of GMM+UU broth and incubated for 24 hours at 37°C. Coverslips were then incubated with GMM+UU or GMM+UU+caspofungin (1 µg/ml) for 2 hours at 37°C. To examine the damage of mature hyphae, coverslips were washed with 4 mL PIPES (pH 6.7) for 5 minutes. PIPES was then removed and washed again with 4 mL PIPES for 5 minutes. After removing the second PIPES wash, 500 uL of propidium iodide (PI) solution (12.5 ug/mL in 50 mM PIPES) was added on top of the coverslip and let incubate in the dark for 5 minutes. Slides were washed in 4 mL PIPES twice as described previously. They were then prepared for microscopy and imaged on an Inverted Leica DMi8 with Leica K5 Microscope Camera using a 10x objective. Images were analyzed in imageJ [72].

Neutropenic murine model of Invasive Aspergillosis:

Murine experiments followed previously established intranasal neutropenic models of IA [73,74]. Sixty 6-week old male CD1 mice (Charles River Laboratories, Raleigh, NC) were injected via intraperitoneal route with 175 mg/kg cyclophosphamide on days −2 and +3 and 40mg/kg triamcinolone acetonide subcutaneously on days −1 and + 6. Twenty mice per strain were infected intranasally with 40 µl of 10^8 spores/ml conidia suspension of the *akuB*^{KU80}, Δ*aspB*, or Δ*aspB::aspB* strains on day +0. On days +1 through +4, mice were injected via intraperitoneal route with either 2 mg/kg caspofungin or saline. Mice were monitored until day +14 and humanely euthanized if they showed severe symptoms. Survival was plotted on a Kaplan-Meier curve with a log rank pair-wise comparison. Murine experiments were conducted in compliance with the SIU Institutional Animal Care and Use Committee Protocol 20-034.

Histopathology Analysis:

Mice were immunocompromised and treated as described above in [Section: *Neutropenic murine model of Invasive Aspergillosis*]. Lungs were harvested on day +3 after infection and tissue sections were stained using hematoxylin and eosin (H&E) stains to visualize inflammation and Gomori's methenamine silver stain to visualize fungal hyphae.

Protein extraction, AspB-eGFP fusion protein purification, and LC-MS/MS Analysis

The *aspB-egfp* strain from [24] was grown in GMM liquid media and GMM liquid media supplemented with 1 µg/mL of caspofungin for 24 hours at 37°C. Protein extraction and pulldown were completed as described by [31,75]. Fungal mycelia were homogenized to obtain total cell lysate and AspB complexes were purified using the GFP-Trap® affinity purification (Chromotek), as described [75]. GFP-Trap® magnetic beads were equilibrated by washing beads three times in 500 µl ice-cold dilution buffer then resuspended in 100 µl ice cold dilution buffer. The resin suspension is then mixed with total cell lysate (10 mg total protein) and incubated at 4°C with gentle agitation for 2 hours. Beads were collected using a magnetic stand. Beads were washed in 500 µl ice-cold lysis buffer and five times with 500 µl of wash buffer. Beads were suspended in 50 µl wash buffer.

Samples were digested on-bead with trypsin followed by C18 desalting. Samples were analyzed via LC-MS/MS on a Thermo Easy nLC 1200-QExactive HF in technical duplicate. All mass spectra data was processed using MaxQuant (ver. 1.6.12.0) and searched against the Uniprot *Aspergillus fumigatus* proteome reviewed database (Proteome ID UP000002530). MaxQuant output was further processed via Perseus with filtering at 1% false discovery rate (FDR). Only proteins with >1 peptide were reported.

Prioritization of candidate genes and generation of deletion mutants

Candidate genes were chosen by prioritizing proteins with at least a two-fold increase, statistical significance, and known or putative roles in cell wall functions as listed in FungiFun GO term search for biological processes (Table S3) [32]. Deletions of *bgt1* (*Afu1g11460*; fungidb.org), *gel1* (*Afu2g01170*; fungidb.org), *gel2* (*Afu6g11390*; fungidb.org), *nsdD* (*Afu3g13870*; fungidb.org), *mapA* (*Afu4g06930*; fungidb.org), and *punA* (*Afu6g07470*; fungidb.org) genes were obtained by replacing the gene with the 2.4 kb *pyrG* gene from *Aspergillus parasiticus*. Approximately 1 kb of promoter and terminator region of each gene were PCR-amplified from AF293 genomic DNA. Deletion constructs were generated by overlap fusion PCR and subsequently transformed into *akuB*^{KU80} *pyrG*− strain, all as previously described by [73]. Primers used in transformation of all candidate strains are found in (Table S2). Transformants were validated via PCR screening.

Acknowledgments:

R.J.B. was supported by the Southern Illinois University Carbondale Master's Fellowship. R.J.B. and J.V.M. were supported in part by 1R01AI165656-01A1. We also want to thank the members of the Vargas-Muñiz group for critical reading of the manuscript. We want to thank Stacey Mcgee (histology core facility) and Dr. Jennifer Harris (SIU Laboratory Animal Program Director) for providing guidance and support during animal experiments.

599 **References:**

600 1. Bongomin F, Gago S, Oladele R, Denning D. Global and Multi-National Prevalence of
601 Fungal Diseases—Estimate Precision. Journal of Fungi. 2017;3: 57.
602 doi:10.3390/jof3040057

603 2. Latgé J-P, Chamilos G. Aspergillus fumigatus and Aspergillosis in 2019. Clin Microbiol
604 Rev. 2019;33. doi:10.1128/CMR.00140-18

605 3. Rybak JM, Fortwendel JR, Rogers PD. Emerging threat of triazole-resistant Aspergillus
606 fumigatus. Journal of Antimicrobial Chemotherapy. 2019;74: 835–842.
607 doi:10.1093/jac/dky517

608 4. Li X, Lau SK, Woo PC. Fungal infection risks associated with the use of cytokine
609 antagonists and immune checkpoint inhibitors. Exp Biol Med. 2020;245: 1104–1114.
610 doi:10.1177/1535370220939862

611 5. Baddley JW. Clinical risk factors for invasive aspergillosis. Med Mycol. 2011;49: S7–S12.
612 doi:10.3109/13693786.2010.505204

613 6. Gouzien L, Cocherie T, Eloy O, Legriel S, Bedos J-P, Simon C, et al. Invasive
614 Aspergillosis associated with Covid-19: A word of caution. Infect Dis Now. 2021;51: 383–
615 386. doi:10.1016/j.idnow.2020.12.008

616 7. Benedict K, Jackson BR, Chiller T, Beer KD. Estimation of Direct Healthcare Costs of
617 Fungal Diseases in the United States. Clinical Infectious Diseases. 2019;68: 1791–1797.
618 doi:10.1093/cid/ciy776

619 8. Dagenais TRT, Keller NP. Pathogenesis of Aspergillus fumigatus in Invasive
620 Aspergillosis. Clin Microbiol Rev. 2009;22: 447–465. doi:10.1128/CMR.00055-08

9. Shlezinger N, Irmer H, Dhingra S, Beattie SR, Cramer RA, Braus GH, et al. Sterilizing immunity in the lung relies on targeting fungal apoptosis-like programmed cell death. Science (1979). 2017;357: 1037–1041. doi:10.1126/science.aan0365

10. Latgé J-P. Aspergillus fumigatus and Aspergillosis. Clin Microbiol Rev. 1999;12: 310–350. doi:10.1128/CMR.12.2.310

11. Morgan J, Wannemuehler KA, Marr KA, Hadley S, Kontoyiannis DP, Walsh TJ, et al. Incidence of invasive aspergillosis following hematopoietic stem cell and solid organ transplantation: interim results of a prospective multicenter surveillance program. Med Mycol. 2005;43: 49–58. doi:10.1080/13693780400020113

12. Balloy V, Huerre M, Latgé J-P, Chignard M. Differences in Patterns of Infection and Inflammation for Corticosteroid Treatment and Chemotherapy in Experimental Invasive Pulmonary Aspergillosis. Infect Immun. 2005;73: 494–503. doi:10.1128/IAI.73.1.494-503.2005

13. Stergiopoulou T, Meletiadis J, Roilides E, Kleiner DE, Schaufele R, Roden M, et al. Host-Dependent Patterns of Tissue Injury in Invasive Pulmonary Aspergillosis. Am J Clin Pathol. 2007;127: 349–355. doi:10.1309/UJRV9DLC11RM3G8R

14. Coutinho AE, Chapman KE. The anti-inflammatory and immunosuppressive effects of glucocorticoids, recent developments and mechanistic insights. Mol Cell Endocrinol. 2011;335: 2–13. doi:10.1016/j.mce.2010.04.005

15. Cain DW, Cidlowski JA. Immune regulation by glucocorticoids. Nat Rev Immunol. 2017;17: 233–247. doi:10.1038/nri.2017.1

16. Patterson TF, Thompson GR, Denning DW, Fishman JA, Hadley S, Herbrecht R, et al. Practice Guidelines for the Diagnosis and Management of Aspergillosis: 2016 Update by

644 the Infectious Diseases Society of America. Clinical Infectious Diseases. 2016;63: e1–
645 e60. doi:10.1093/cid/ciw326

646 17. World Health Organization. WHO fungal priority pathogens list to guide research,
647 development and public health action. 2022. Available:
648 https://www.who.int/publications/i/item/9789240060241

649 18. Denning DW. Echinocandin antifungal drugs. The Lancet. 2003;362: 1142–1151.
650 doi:10.1016/S0140-6736(03)14472-8

651 19. Dudiuk C, Berrio I, Leonardelli F, Morales-Lopez S, Theill L, Macedo D, et al. Antifungal
652 activity and killing kinetics of anidulafungin, caspofungin and amphotericin B against
653 Candida auris. Journal of Antimicrobial Chemotherapy. 2019;74: 2295–2302.
654 doi:10.1093/jac/dkz178

655 20. Lewis JS, Graybill JR. Fungicidal versus Fungistatic: what's in a word? Expert Opin
656 Pharmacother. 2008;9: 927–935. doi:10.1517/14656566.9.6.927

657 21. Graybill JR, Burgess DS, Hardin TC. Key issues concerning fungistatic versus fungicidal
658 drugs. European Journal of Clinical Microbiology & Infectious Diseases. 1997;16: 42–50.
659 doi:10.1007/BF01575120

660 22. Hiemenz JW, Raad II, Maertens JA, Hachem RY, Saah AJ, Sable CA, et al. Efficacy of
661 caspofungin as salvage therapy for invasive aspergillosis compared to standard therapy
662 in a historical cohort. European Journal of Clinical Microbiology & Infectious Diseases.
663 2010;29: 1387–1394. doi:10.1007/s10096-010-1013-0

664 23. Mela A, Momany M. Septins coordinate cell wall integrity and lipid metabolism in a
665 sphingolipid-dependent process. J Cell Sci. 2022;135. doi:10.1242/jcs.258336

24. Vargas-Muñiz JM, Renshaw H, Richards AD, Lamoth F, Soderblom EJ, Moseley MA, et al. The Aspergillus fumigatus septins play pleiotropic roles in septation, conidiation, and cell wall stress, but are dispensable for virulence. Fungal Genetics and Biology. 2015;81: 41–51. doi:10.1016/j.fgb.2015.05.014

25. Juvvadi PR, Fortwendel JR, Rogg LE, Steinbach WJ. Differential localization patterns of septins during growth of the human fungal pathogen Aspergillus fumigatus reveal novel functions. Biochem Biophys Res Commun. 2011;405: 238–243. doi:10.1016/j.bbrc.2011.01.017

26. Bertin A, McMurray MA, Grob P, Park S-S, Garcia G, Patanwala I, et al. Saccharomyces cerevisiae septins: Supramolecular organization of heterooligomers and the mechanism of filament assembly. Proceedings of the National Academy of Sciences. 2008;105: 8274–8279. doi:10.1073/pnas.0803330105

27. Shuman B, Momany M. Septins From Protists to People. Front Cell Dev Biol. 2022;9. doi:10.3389/fcell.2021.824850

28. Badrane H, Nguyen MH, Blankenship JR, Cheng S, Hao B, Mitchell AP, et al. Rapid Redistribution of Phosphatidylinositol-(4,5)-Bisphosphate and Septins during the Candida albicans Response to Caspofungin. Antimicrob Agents Chemother. 2012;56: 4614–4624. doi:10.1128/AAC.00112-12

29. Badrane H, Nguyen MH, Clancy CJ. Highly Dynamic and Specific Phosphatidylinositol 4,5-Bisphosphate, Septin, and Cell Wall Integrity Pathway Responses Correlate with Caspofungin Activity against Candida albicans. Antimicrob Agents Chemother. 2016;60: 3591–3600. doi:10.1128/AAC.02711-15

30. Wagner AS, Lumsdaine SW, Mangrum MM, Reynolds TB. Caspofungin-induced β(1,3)-glucan exposure in Candida albicans is driven by increased chitin levels. mBio. 2023. doi:10.1128/mbio.00074-23

31. Vargas-Muñiz JM, Renshaw H, Waitt G, Soderblom EJ, Moseley MA, Palmer JM, et al. Caspofungin exposure alters the core septin AspB interactome of Aspergillus fumigatus. Biochem Biophys Res Commun. 2017;485: 221–226. doi:10.1016/j.bbrc.2017.02.116

32. Priebe S, Linde J, Albrecht D, Guthke R, Brakhage AA. FungiFun: A web-based application for functional categorization of fungal genes and proteins. Fungal Genetics and Biology. 2011;48: 353–358. doi:10.1016/j.fgb.2010.11.001

33. HARTWELL L. Genetic control of the cell division cycle in yeast *1IV. Genes controlling bud emergence and cytokinesis. Exp Cell Res. 1971;69: 265–276. doi:10.1016/0014-4827(71)90223-0

34. Gladfelter A. The septin cortex at the yeast mother-bud neck. Curr Opin Microbiol. 2001;4: 681–689. doi:10.1016/S1369-5274(01)00269-7

35. McMurray MA, Thorner J. Septins: molecular partitioning and the generation of cellular asymmetry. Cell Div. 2009;4: 18. doi:10.1186/1747-1028-4-18

36. Blankenship JR, Fanning S, Hamaker JJ, Mitchell AP. An Extensive Circuitry for Cell Wall Regulation in Candida albicans. PLoS Pathog. 2010;6: e1000752. doi:10.1371/journal.ppat.1000752

37. DeMarini DJ, Adams AEM, Fares H, Virgilio C De, Valle G, Chuang JS, et al. A Septin-based Hierarchy of Proteins Required for Localized Deposition of Chitin in the Saccharomyces cerevisiae Cell Wall. J Cell Biol. 1997;139: 75–93. doi:10.1083/jcb.139.1.75

711 38. Fukuda K, Yamada K, Deoka K, Yamashita S, Ohta A, Horiuchi H. Class III Chitin
712 Synthase ChsB of Aspergillus nidulans Localizes at the Sites of Polarized Cell Wall
713 Synthesis and Is Required for Conidial Development. Eukaryot Cell. 2009;8: 945–956.
714 doi:10.1128/EC.00326-08

715 39. Hernández-Rodríguez Y, Masuo S, Johnson D, Orlando R, Smith A, Couto-Rodriguez M,
716 et al. Distinct Septin Heteropolymers Co-Exist during Multicellular Development in the
717 Filamentous Fungus Aspergillus nidulans. PLoS One. 2014;9: e92819.
718 doi:10.1371/journal.pone.0092819

719 40. Martinez Barrera S, Hatchell E, Byrum SD, Mackintosh SG, Kozubowski L. Quantitative
720 analysis of septin Cdc10 & Cdc3-associated proteome during stress response in the
721 fungal pathogen Cryptococcus neoformans. PLoS One. 2024;19: e0313444.
722 doi:10.1371/journal.pone.0313444

723 41. Ben-Ami R. Systemic Antifungal Therapy for Invasive Pulmonary Infections. Journal of
724 Fungi. 2023;9: 144. doi:10.3390/jof9020144

725 42. Syed YY. Rezafungin: First Approval. Drugs. 2023;83: 833–840. doi:10.1007/s40265-
726 023-01891-8

727 43. Perlin DS. Current perspectives on echinocandin class drugs. Future Microbiol. 2011;6:
728 441–457. doi:10.2217/fmb.11.19

729 44. Fortwendel JR, Juvvadi PR, Perfect BZ, Rogg LE, Perfect JR, Steinbach WJ.
730 Transcriptional Regulation of Chitin Synthases by Calcineurin Controls Paradoxical
731 Growth of Aspergillus fumigatus in Response to Caspofungin. Antimicrob Agents
732 Chemother. 2010;54: 1555–1563. doi:10.1128/AAC.00854-09

45. Juvvadi PR, Muñoz A, Lamoth F, Soderblom EJ, Moseley MA, Read ND, et al. Calcium-Mediated Induction of Paradoxical Growth following Caspofungin Treatment Is Associated with Calcineurin Activation and Phosphorylation in Aspergillus fumigatus. Antimicrob Agents Chemother. 2015;59: 4946–4955. doi:10.1128/AAC.00263-15

46. Iwase M, Okada S, Oguchi T, Toh-e A. Forchlorfenuron, a phenylurea cytokinin, disturbs septin organization in Saccharomyces cerevisiae. Genes Genet Syst. 2004;79: 199–206. doi:10.1266/ggs.79.199

47. Hu Q, Nelson WJ, Spiliotis ET. Forchlorfenuron Alters Mammalian Septin Assembly, Organization, and Dynamics. Journal of Biological Chemistry. 2008;283: 29563–29571. doi:10.1074/jbc.M804962200

48. Angelis D, Karasmanis EP, Bai X, Spiliotis ET. In Silico Docking of Forchlorfenuron (FCF) to Septins Suggests that FCF Interferes with GTP Binding. PLoS One. 2014;9: e96390. doi:10.1371/journal.pone.0096390

49. Kim KK, Singh RK, Khazan N, Kodza A, Singh NA, Jones A, et al. Development of Potent Forchlorfenuron Analogs and Their Cytotoxic Effect in Cancer Cell Lines. Sci Rep. 2020;10: 3241. doi:10.1038/s41598-020-59824-4

50. Beauvais A, Latgé J-P. Membrane and cell wall targets in Aspergillus fumigatus. Drug Resistance Updates. 2001;4: 38–49. doi:10.1054/drup.2001.0185

51. Gastebois A, Mouyna I, Simenel C, Clavaud C, Coddeville B, Delepierre M, et al. Characterization of a New β(1–3)-Glucan Branching Activity of Aspergillus fumigatus. Journal of Biological Chemistry. 2010;285: 2386–2396. doi:10.1074/jbc.M109.077545

754 52. Sarthy A V., McGonigal T, Coen M, Frost DJ, Meulbroek JA, Goldman RC. Phenotype in
755 Candida albicans of a disruption of the BGL2 gene encoding a 1,3-β-glucosyltransferase.
756 Microbiology (N Y). 1997;143: 367–376. doi:10.1099/00221287-143-2-367

757 53. Kalebina TS, Farkaš V, Laurinavichiute DK, Gorlovoy PM, Fominov G V., Bartek P, et al.
758 Deletion of BGL2 results in an increased chitin level in the cell wall of Saccharomyces
759 cerevisiae . Antonie Van Leeuwenhoek. 2003;84: 179–184.
760 doi:10.1023/A:1026034123673

761 54. Millet N, Latgé J-P, Mouyna I. Members of Glycosyl-Hydrolase Family 17 of A. fumigatus
762 Differentially Affect Morphogenesis. Journal of Fungi. 2018;4: 18. doi:10.3390/jof4010018

763 55. Zhao W, Lu Y, Ouyang H, Zhou H, Yan J, Du T, et al. N-Glycosylation of Gel1 or Gel2 is
764 vital for cell wall-glucan synthesis in Aspergillus fumigatus. Glycobiology. 2013;23: 955–
765 968. doi:10.1093/glycob/cwt032

766 56. Mouyna I, Morelle W, Vai M, Monod M, Léchenne B, Fontaine T, et al. Deletion of GEL2
767 encoding for a β(1–3)glucanosyltransferase affects morphogenesis and virulence in
768 Aspergillus fumigatus. Mol Microbiol. 2005;56: 1675–1688. doi:10.1111/j.1365-
769 2958.2005.04654.x

770 57. Große V, Krappmann S. The Asexual Pathogen Aspergillus fumigatus Expresses
771 Functional Determinants of Aspergillus nidulans Sexual Development. Eukaryot Cell.
772 2008;7: 1724–1732. doi:10.1128/EC.00157-08

773 58. Han K-H, Han K-Y, Yu J-H, Chae K-S, Jahng K-Y, Han D-M. The nsdD gene encodes a
774 putative GATA-type transcription factor necessary for sexual development of Aspergillus
775 nidulans. Mol Microbiol. 2001;41: 299–309. doi:10.1046/j.1365-2958.2001.02472.x

776 59. O'Gorman CM, Fuller HT, Dyer PS. Discovery of a sexual cycle in the opportunistic
777 fungal pathogen Aspergillus fumigatus. Nature. 2009;457: 471–474.
778 doi:10.1038/nature07528

779 60. Szewczyk E, Krappmann S. Conserved Regulators of Mating Are Essential for
780 Aspergillus fumigatus Cleistothecium Formation. Eukaryot Cell. 2010;9: 774–783.
781 doi:10.1128/EC.00375-09

782 61. Li X, Chang YH. Amino-terminal protein processing in Saccharomyces cerevisiae is an
783 essential function that requires two distinct methionine aminopeptidases. Proceedings of
784 the National Academy of Sciences. 1995;92: 12357–12361.
785 doi:10.1073/pnas.92.26.12357

786 62. Brown JA, Sherlock G, Myers CL, Burrows NM, Deng C, Wu HI, et al. Global analysis of
787 gene function in yeast by quantitative phenotypic profiling. Mol Syst Biol. 2006;2.
788 doi:10.1038/msb4100043

789 63. Lanze CE, Gandra RM, Foderaro JE, Swenson KA, Douglas LM, Konopka JB. Plasma
790 Membrane MCC/Eisosome Domains Promote Stress Resistance in Fungi. Microbiology
791 and Molecular Biology Reviews. 2020;84. doi:10.1128/MMBR.00063-19

792 64. Grossmann G, Malinsky J, Stahlschmidt W, Loibl M, Weig-Meckl I, Frommer WB, et al.
793 Plasma membrane microdomains regulate turnover of transport proteins in yeast. J Cell
794 Biol. 2008;183: 1075–1088. doi:10.1083/jcb.200806035

795 65. Hosiner D, Sponder G, Graschopf A, Reipert S, Schweyen RJ, Schüller C, et al. Pun1p is
796 a metal ion-inducible, calcineurin/Crz1p-regulated plasma membrane protein required for
797 cell wall integrity. Biochimica et Biophysica Acta (BBA) - Biomembranes. 2011;1808:
798 1108–1119. doi:10.1016/j.bbamem.2011.01.002

66. Mir SS, Fiedler D, Cashikar AG. Ssd1 Is Required for Thermotolerance and Hsp104-Mediated Protein Disaggregation in Saccharomyces cerevisiae. Mol Cell Biol. 2009;29: 187–200. doi:10.1128/MCB.02271-07

67. Xu T, Shively CA, Jin R, Eckwahl MJ, Dobry CJ, Song Q, et al. A Profile of Differentially Abundant Proteins at the Yeast Cell Periphery during Pseudohyphal Growth. Journal of Biological Chemistry. 2010;285: 15476–15488. doi:10.1074/jbc.M110.114926

68. Alvarez FJ, Douglas LM, Rosebrock A, Konopka JB. The Sur7 Protein Regulates Plasma Membrane Organization and Prevents Intracellular Cell Wall Growth in Candida albicans. Mol Biol Cell. 2008;19: 5214–5225. doi:10.1091/mbc.e08-05-0479

69. Ferreira ME da S, Malavazi I, Savoldi M, Brakhage AA, Goldman MHS, Kim HS, et al. Transcriptome analysis of Aspergillus fumigatus exposed to voriconazole. Curr Genet. 2006;50: 32–44. doi:10.1007/s00294-006-0073-2

70. da Silva Ferreira ME, Kress MRVZ, Savoldi M, Goldman MHS, Ha□rtl A, Heinekamp T, et al. The akuBKU80 Mutant Deficient for Nonhomologous End Joining Is a Powerful Tool for Analyzing Pathogenicity in Aspergillus fumigatus. Eukaryot Cell. 2006;5: 207–211. doi:10.1128/EC.5.1.207-211.2006

71. Fortwendel JR, Juvvadi PR, Pinchai N, Perfect BZ, Alspaugh JA, Perfect JR, et al. Differential effects of inhibiting chitin and 1,3-β-D-glucan synthesis in ras and calcineurin mutants of Aspergillus fumigatus. Antimicrob Agents Chemother. 2009;53: 476–482. doi:10.1128/AAC.01154-08

72. Bourne R. ImageJ. Fundamentals of Digital Imaging in Medicine. London: Springer London; 2010. pp. 185–188. doi:10.1007/978-1-84882-087-6_9

73. Steinbach WJ, Cramer RA, Perfect BZ, Asfaw YG, Sauer TC, Najvar LK, et al. Calcineurin Controls Growth, Morphology, and Pathogenicity in Aspergillus fumigatus. Eukaryot Cell. 2006;5: 1091–1103. doi:10.1128/EC.00139-06

74. Steinbach WJ, Benjamin Jr DK, Trasi SA, Miller JL, Schell WA, Zaas AK, et al. Value of an inhalational model of invasive aspergillosis. Med Mycol. 2004;42: 417–425. doi:10.1080/13693780410001712034

75. Juvvadi PR, Belina D, Soderblom EJ, Moseley MA, Steinbach WJ. Filamentous fungal-specific septin AspE is phosphorylated in vivo and interacts with actin, tubulin and other septins in the human pathogen Aspergillus fumigatus. Biochem Biophys Res Commun. 2013;431: 547–553. doi:10.1016/j.bbrc.2013.01.020

Figures:

Fig 1. AspA, AspB, and AspC are involved in fungal response to caspofungin. The deletion of *aspA, aspB, and aspC* results in reduction of viability to echinocandins. (A) Spore dilution assay show an increase in susceptibility to caspofungin in the Δ*aspA,* Δ*aspB,* and Δ*aspC* strains. 10^4-10^1 conidia were plated on GMM media supplemented with caspofungin for 48 hours at 37°C. (B, C) Deletion of *aspB* results in loss of viability when grown in caspofungin but not micafungin. 10^4 conidia were incubated for 48 hours in GMM supplemented with (B) 1µg/mL caspofungin or (C) 1 µg/mL micafungin. Cells were incubated in CFDA for one hour then visualized. Viable and non-viable colonies were counted. The number of viable colonies was divided by the total number of colonies. Experiment was replicated three times. Error bar represent SEM. Student t-test were done in Graphpad Prism, with each strain compared against the *akuB*^{KU80} wild-type. (D) E-strip plates of caspofungin and micafungin show clearer zone of effect in Δ*aspA,* Δ*aspB*, and Δ*aspC* strains. 10^6 conidia were plated with beads and left to dry. E-strip was placed, and

plates were grown at 37°C for 48 hours. All experiments were replicated three times. Representative images are shown in this figure.

Fig 2. Δ*aspB* strain loses cell viability when grown in caspofungin. (A) All strains had viability when grown in GMM+UU. 10^4 conidia were grown in 4 mL GMM+UU at 37°C for 24 hours. Cells were then treated with CFDA, which is hydrolyzed in living cells to a fluorescent ester, then visualized. (B) Loss of viability in Δ*aspB* strain is seen after growth in the presence of caspofungin. After 48 hours post exposure to 1 µg/mL caspofungin, cells were incubated in CFDA for one hour then visualized. Experiments were replicated three times. Scale bar is 500 µm.

Fig 3. Δ*aspB* strain has increased hyphal damage during caspofungin exposure.

(A) No hyphal damage seen in basal conditions. 10^4 conidia were grown in GMM at 37°C for 24 hours. Cells were then washed with PIPES (pH 6.7) for 5 minutes twice. Slides were then treated with propidium iodide (PI) solution, which stains nucleic acids. Coverslips were washed twice with PIPES, then prepared and visualized. (B) Hyphal damage was seen in Δ*aspB* strain treated with caspofungin. 10^4 conidia were grown in GMM at 37°C for 24 hours. Coverslips were then incubated in caspofungin for 2 hours at 37°C. Cells were then washed with PIPES and treated with PI solution. Experiments were replicated three times. Scale bar is 500 µm.

Fig 4. The Δ*aspB* strain treated with caspofungin has reduced inflammation and fungal burden in immunosuppressed intranasal murine model of invasive aspergillosis.

(A-B) Mice infected with Δ*aspB* strain and treated with caspofungin had a higher chance of survival. Ten mice per strain per condition were infected intranasally with 4×10^6 conidia. Mice

were treated with either saline (A) or caspofungin (B) on days +1 through +4 post-infection. Mice were monitored at least twice a day for 14 days. Survival is on a Kaplan-Meier curve with log rank pair-wise comparison ($p<0.0001$). (C) H&E stain of lungs after 3 days post-infection shows that there is a decrease in inflammatory response in Δ*aspB* infected mice treated with caspofungin. Silver stain shows less and smaller fungal lesions in Δ*aspB* infected mice treated with caspofungin. H&E images taken on an Echo Rebel Hybrid Light microscope using a 10x objective. Scale bar is 300 µm. Silver stain images taken on an Inverted Leica DMi8 with Leica K5 Microscope Camera using a 40x objective. Scale bar is 100 µm.

Fig 5. Δ*nsdD* and Δ*punA* strains have a growth defect; Bgt1, Gel2, NsdD, and MapA are involved in conidiation; and Δ*bgt1*, Δ*gel2*, Δ*nsdD*, and Δ*mapA* strains have septation defects. (A, D) Δ*nsdD* and Δ*punA* have a significant defect in radial growth after 5 days incubation. 10^4 total conidia of each strain were placed on GMM agar. Plates were incubated for 5 days and radial growth was measured every 24 hours. Experiments were replicated three times. (B, E) Deletion of *aspB*, *bgt1*, *gel2*, *nsdD*, or *mapA* results in reduced conidial production. Δ*punA* has increased conidial production. Conidia were collected on day 5 of growth on GMM media using 10 mL of 0.05% Tween-80. Conidia were counted using a hemocytometer and values were divided by the total area of growth to account for strains with growth defects. Experiments were replicated three times. (C) Δ*aspB* and Δ*bgt1* have an increase in length of the apical compartment. Δ*gel2*, Δ*nsdD*, and Δ*mapA* have a decrease in length of the apical compartment. 10^4 total conidia of each strain were inoculated onto coverslips immersed in GMM and incubated for 15 hours. Coverslips were stained with aniline blue and visualized. The length of the apical compartments (N=20) was measured using imageJ. (A, B, C) Experiment performed at 37°C. (D, E) Experiment performed at 30°C. Error bar represent SEM. One-way ANOVA with Tukey's multiple-comparison test were performed in Graphpad Prism and were declared

895 significantly different at a p-value of <0.05. Group means with different lowercase letters are
896 significantly different.

897

898 Fig 6. Deletion of Bgt1, Gel2, NsdD, and MapA increases susceptibility to caspofungin.

899 (A, C) Spore dilution assays show Δ*bgt1*, Δ*gel2*, Δ*nsdD*, and Δ*mapA* strains have an increase in
900 susceptibility to caspofungin. Conidia (10^4-10^1) were grown on GMM media supplemented with
901 1 µg/mL caspofungin for 48 hours. (B, D) Deletion of *bgt1*, *gel2*, *nsdD*, and *mapA* results in
902 reduced, but not loss of, viability when grown in caspofungin. Deletion of *gel1* and *punA* does
903 not affect viability when exposed to caspofungin. 10^4 conidia were grown in GMM for 24 hours
904 then incubated in CFDA and visualized. Experiment was replicated three times. Error bar
905 represent SEM. One-way ANOVA with Tukey's multiple-comparison test were performed in
906 Graphpad Prism and were declared significantly different at a p-value of <0.05. Group means
907 with different lowercase letters are significantly different. (A, B) Experiment performed at 37°C.
908 (C, D) Experiment performed at 30°C.

909

910 Fig 7. Δ*bgt1*, Δ*gel2*, Δ*nsdD*, and Δ*mapA* strains have reduced cell viability when grown in
911 caspofungin. (A, C) All strains were fully viable when grown in GMM media. Conidia (10^4) were
912 grown in GMM for 24 hours on coverslips then incubated in CFDA. Slides were prepared and
913 visualized on an Inverted Leica DMi8 with Leica K5 Microscope Camera using a 10x objective.
914 (B, D) Candidate deletion strains did not lose total viability, but strains Δ*bgt1*, Δ*gel2*, Δ*nsdD*, and
915 Δ*mapA* had a partial reduction in viability. Conidia (10^4) were grown on coverslips immersed in
916 GMM supplemented with 1 µg/mL caspofungin for 48 hours. Coverslips were then incubated in
917 CFDA and visualized. (A, B) Experiment performed at 37°C. (C, D) Experiment performed at
918 30°C. All experiments were replicated three times. Scale bar is 500 µm.

Fig 8. Δ*bgt1*, Δ*gel2*, Δ*nsdD*, and Δ*mapA* strains have increased hyphal damage during caspofungin exposure. (A, C) Hyphal damage was not observed in basal conditions. Conidia (10^4) were grown on coverslips in GMM for 24 hours. Coverslips were washed in PIPES (pH 6.7) for 5 minutes twice then treated with propidium iodide (PI) solution. Coverslips were washed twice with PIPES, then visualized on an Inverted Leica DMi8 with Leica K5 Microscope Camera using a 10x objective. (B, D) Strains Δ*bgt1*, Δ*gel2*, Δ*nsdD*, and Δ*mapA* had hyphal damage when treated with caspofungin. Conidia (10^4) were grown on coverslips in GMM for 24 hours, then incubated in caspofungin for 2 hours. Cells were then washed with PIPES and incubated with PI. (A, B) Experiment performed at 37°C. (C, D) Experiment performed at 30°C. Experiments were replicated three times. Scale bar is 500 µm.

Supplementary Figure 1. Caspofungin exposure alters AspB protein interactions.

(A) Principal component analysis (PCA) of the proteomics data reveals different protein composition from AspB pulldown from GMM and caspofungin treated samples. Blue color denotes those grown in GMM, red color denotes fungi grown in GMM+ 1 µg/mL caspofungin. (B) 226 significantly decreased (FC < -2, $p < 0.05$) proteins (blue) and 106 significantly increased (FC > 2, $p < 0.05$) proteins (red). Proteins under two-fold change or had a p-value greater than 0.05 are shown in black. Red horizontal line denotes p=0.05, red vertical lines denote ± 2 fold change. (C) Category of biological processes most enriched after exposure to caspofungin is hyphal growth. (D) Category of biological processes most decreased after exposure to caspofungin is protein folding. (C,D) Gene ontology enrichment for biological processes determined by using FungiFun [32].

Supplementary Figure 2. Δ*nsdD* and Δ*punA* strains have a growth defect.

Radial growth assay shown per each day, 10^4 conidia of each strain were inoculated on GMM agar. Plates were then incubated for 5 days, and radial growth was measured every 24 hours. (A) Assays performed at 37°C. (B) Assays performed at 30°C. All experiments done in triplicate.

Supplementary Figure 3. Δ*bgt1*, Δ*gel2*, and Δ*nsdD* have mild sensitivity to calcofluor white.

10^4 conidia were inoculated into GMM agar supplemented with cell wall disrupting agents listed in the figure then incubated for 3 days at 37°C, with the exception of 4 µg/mL caspofungin for five days to ensure observation of the caspofungin paradoxical effect. Experiments were replicated three times.

Supplementary Figure 4. Deletion of *punA* results in changed colony morphology in nikkomycin Z.

10^4 conidia were inoculated into GMM agar supplemented with the cell wall disrupting agents listed in the figure then incubated for 3 days at 30°C, with the exception of 4 µg/mL caspofungin for five days to ensure observation of the caspofungin paradoxical effect. Experiments were replicated three times and representative images are shown.

Figure 1

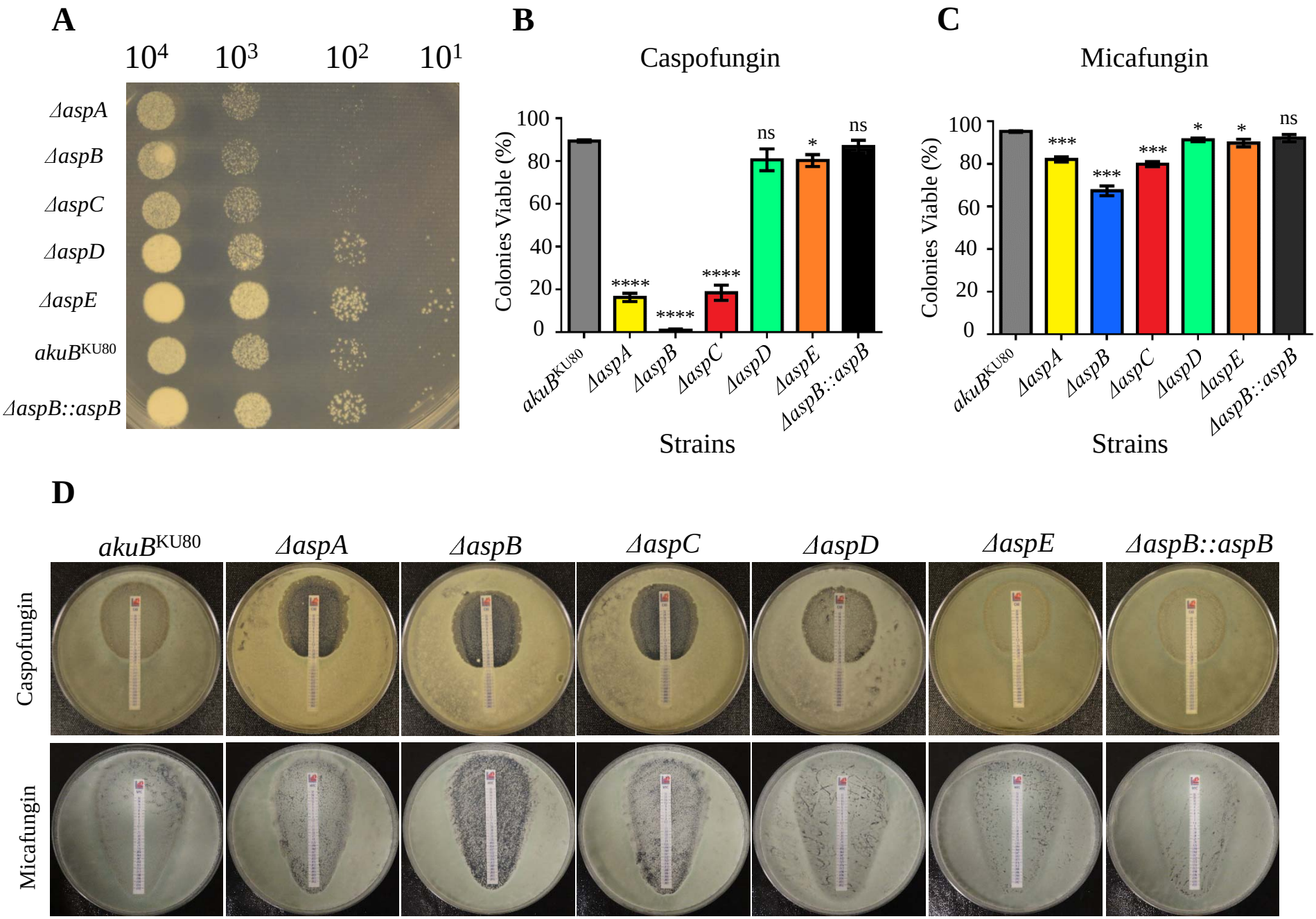

Figure 2

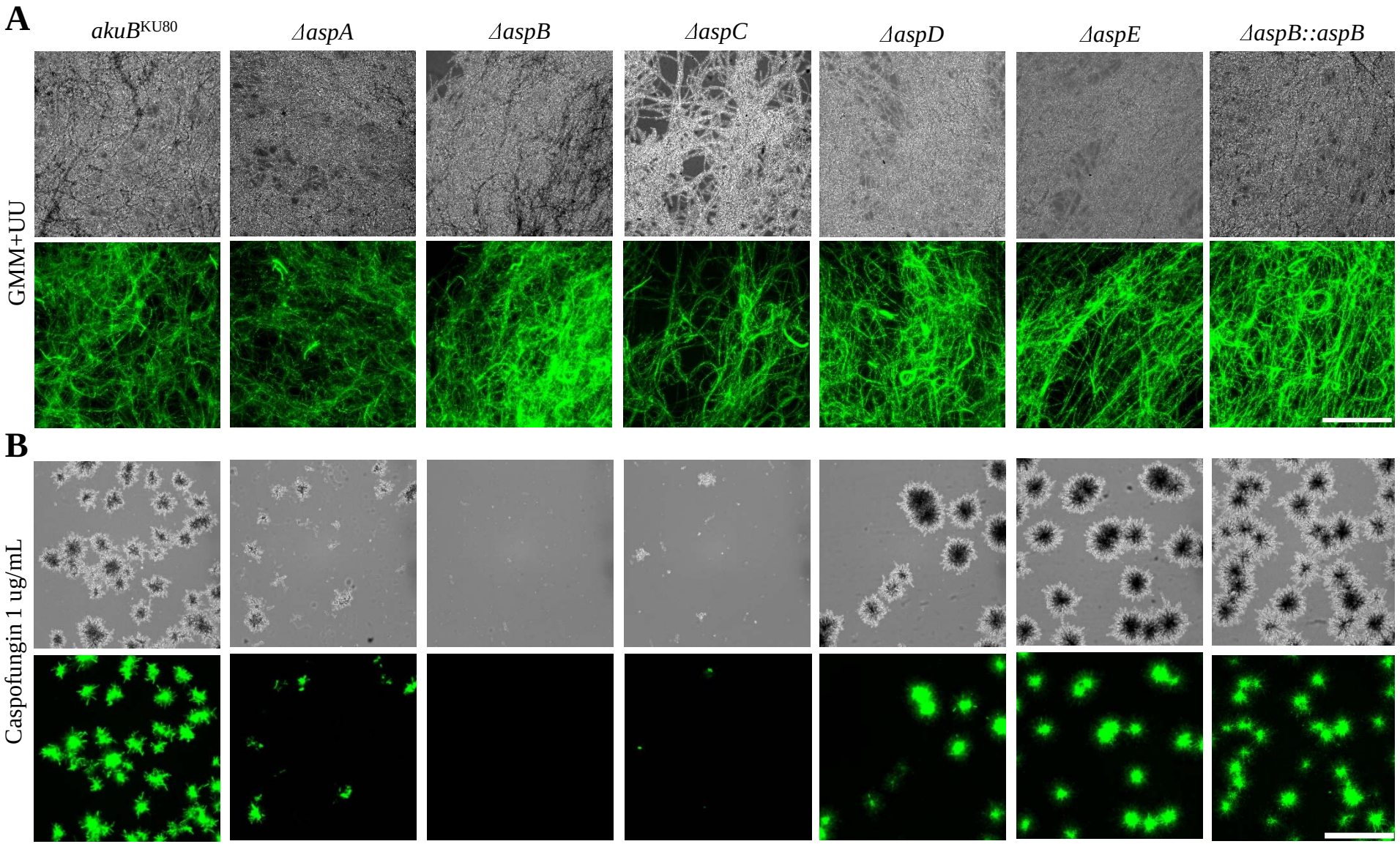

Figure 3

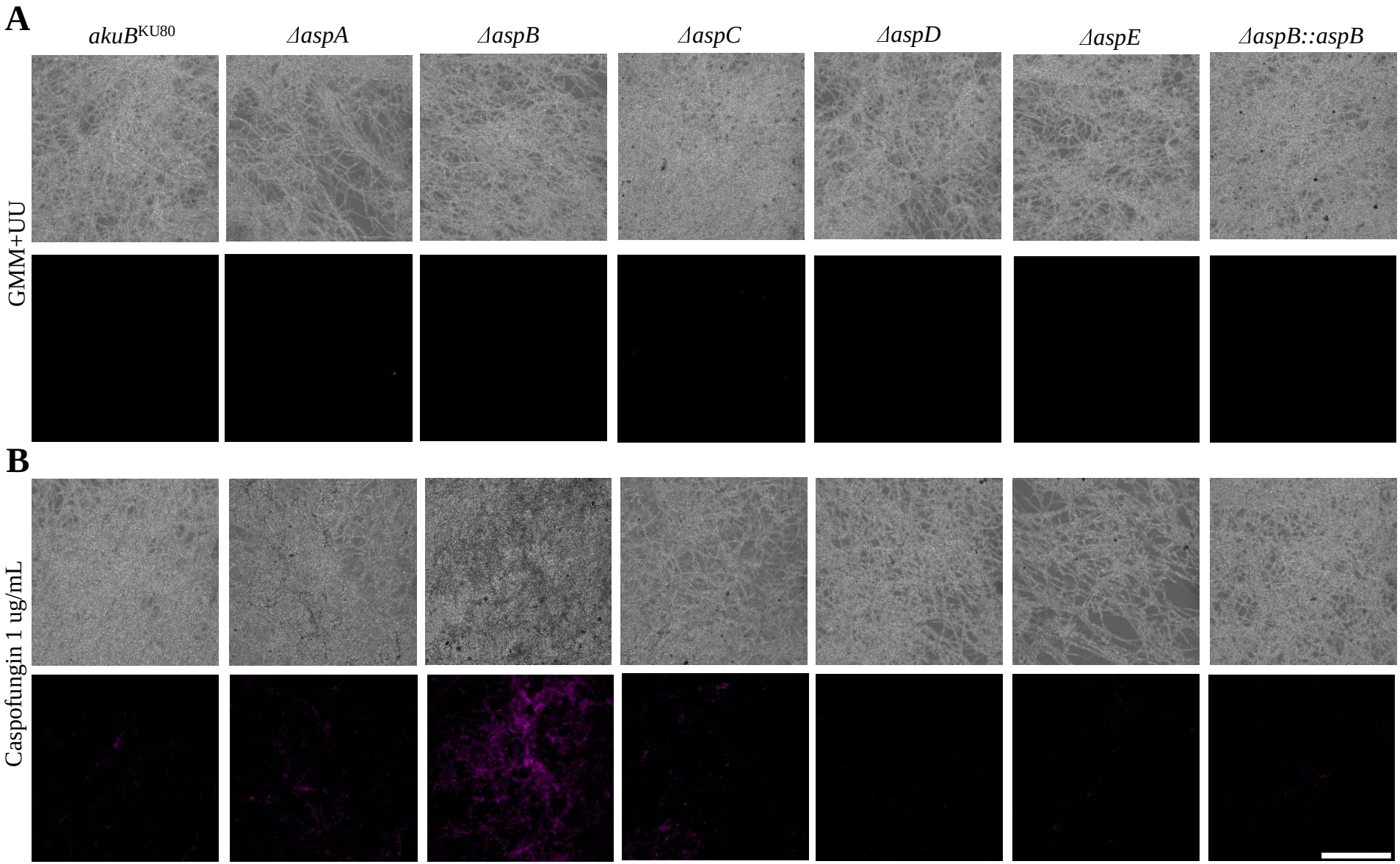

Figure 4

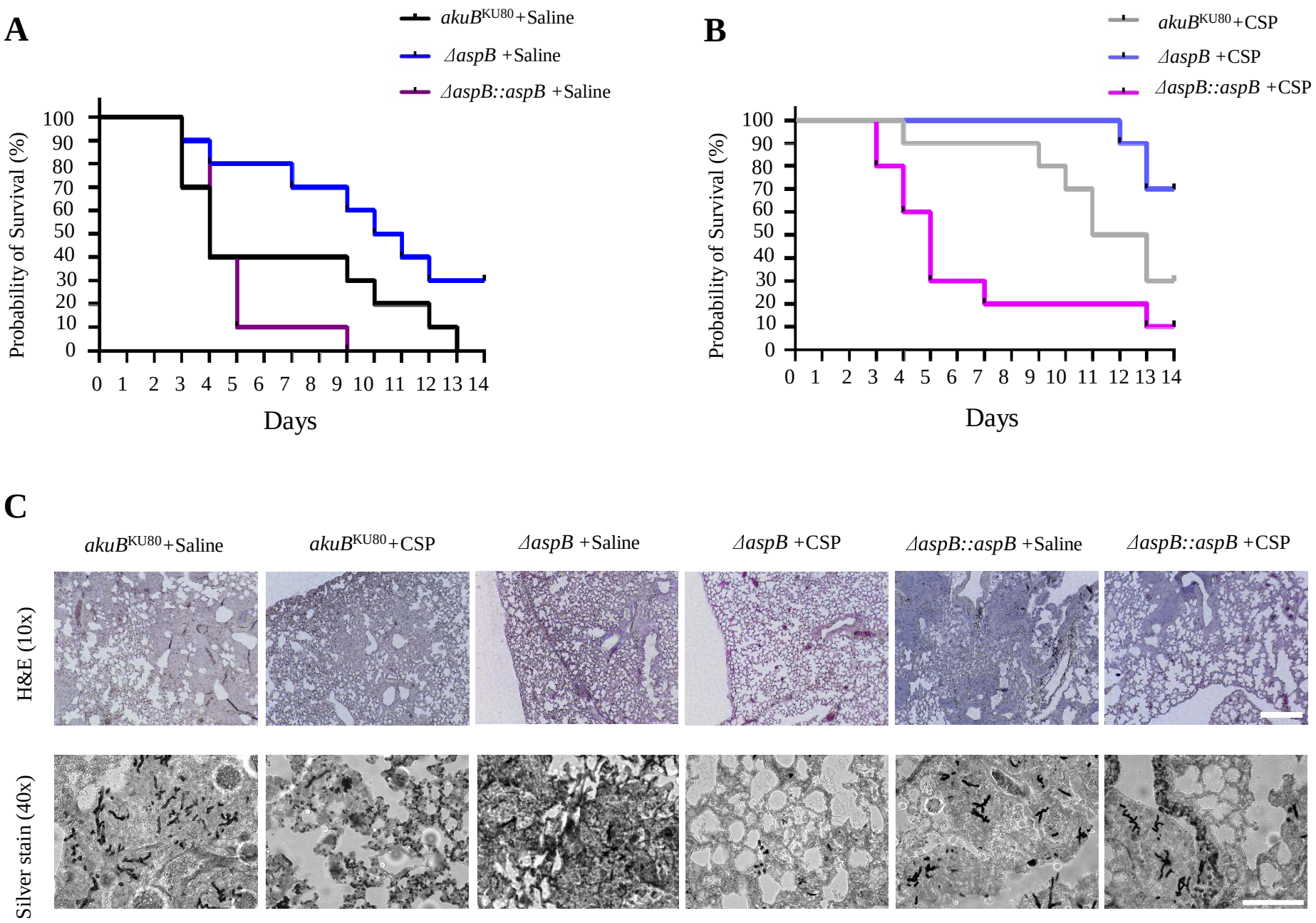

Figure 5

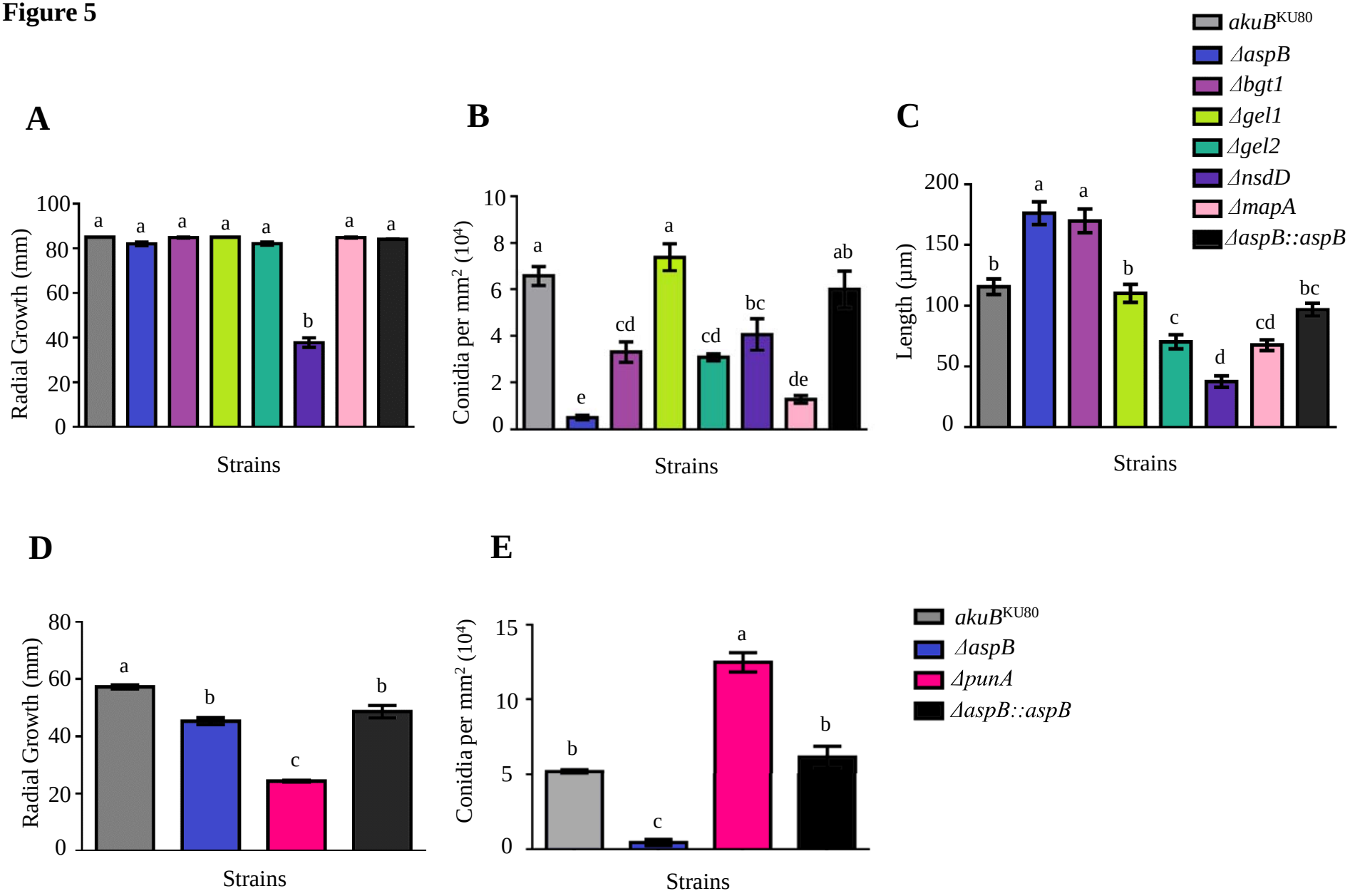

Figure 6

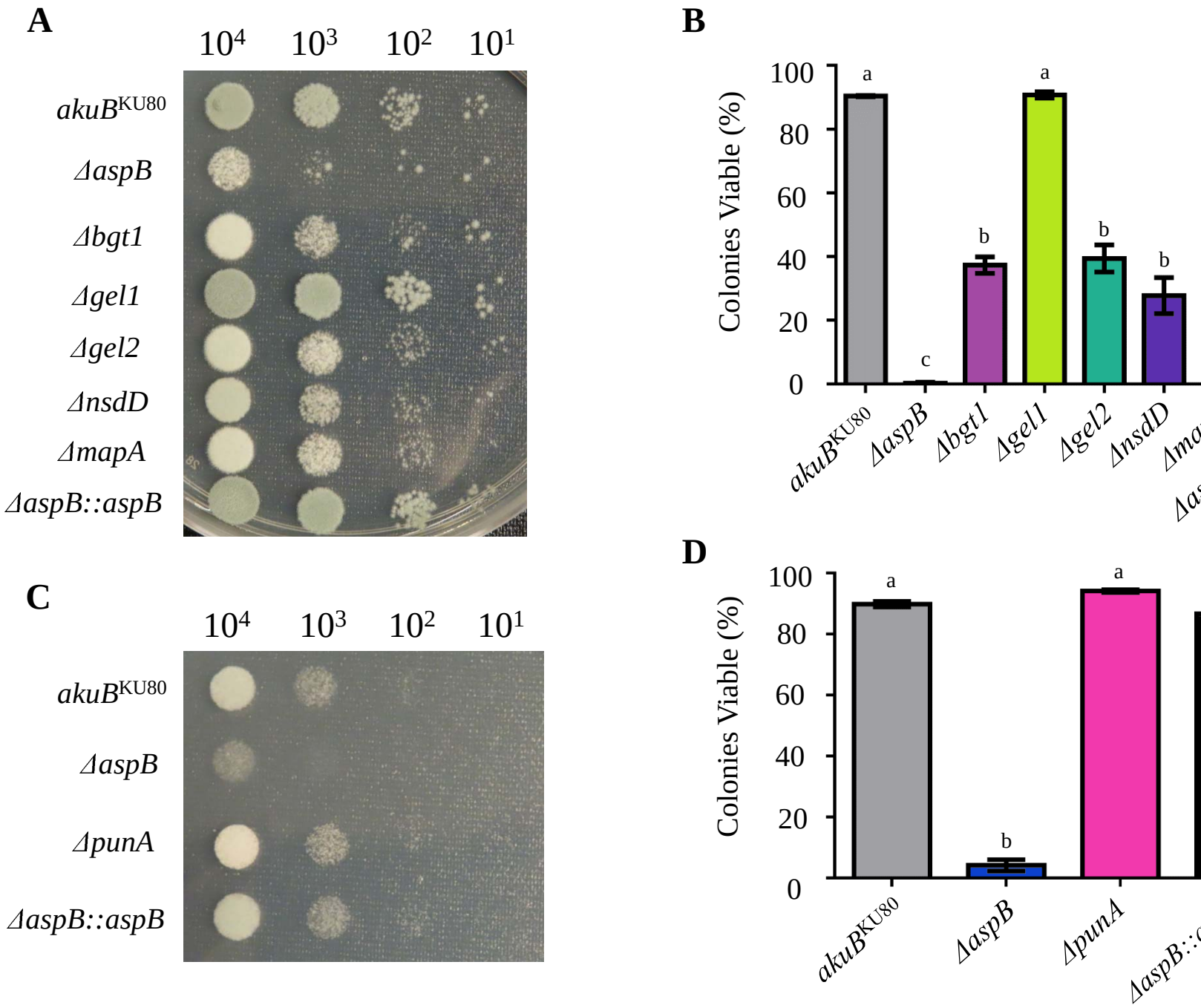

Figure 7

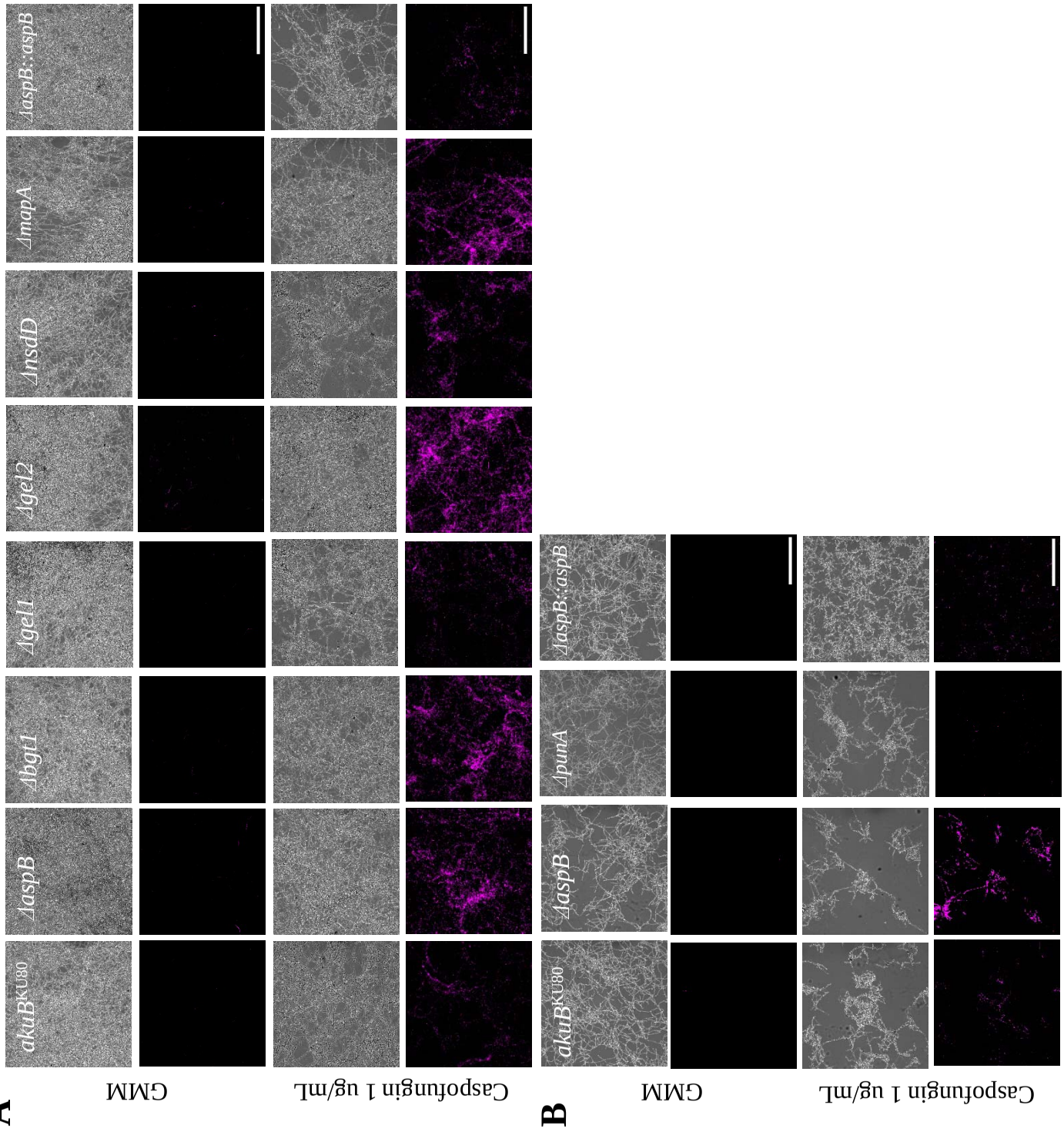

Figure 8

Supplementary Figure 1

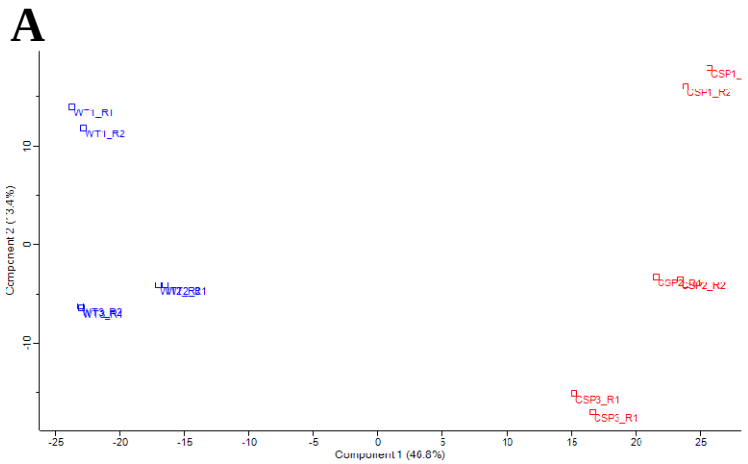

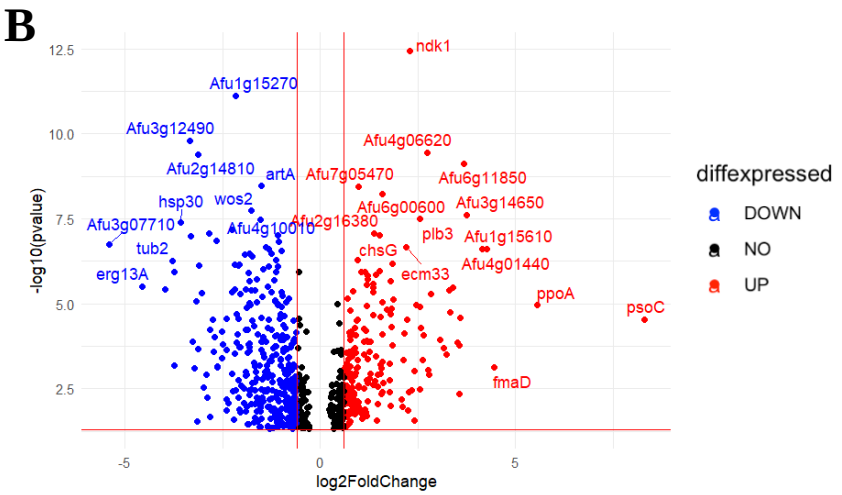

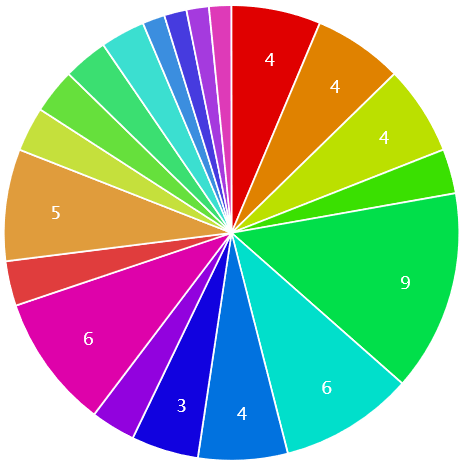

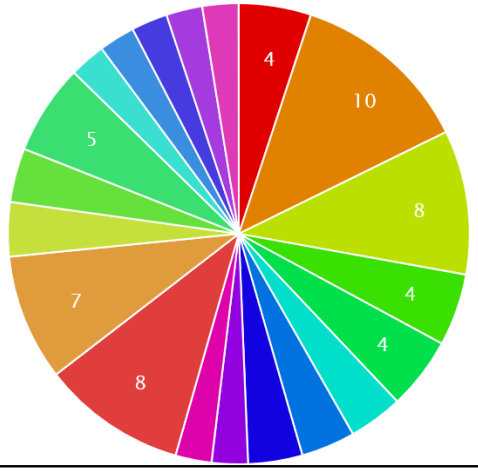

Proteasomal ubiquitin-independent protein catabolic process
Arginine biosynthetic process
Fungal-type cell wall organization
Positive regulation of protein kinase activity
Fumagillin biosynthetic process
Cell separation after cytokinesis
Proteolysis
RNA catabolic process
Chitin localization
Cellular process
Cellular process
Positive regulation of sexual sporulation resulting in formation of a cellular spore
Glucosamine biosynthetic process
Regulation of nitrogen compound metabolic process
Conidiophore development
Branched-chain amino acid catabolic process
Proteasome-mediated ubiquitin-dependent protein catabolic process
Hyphal growth
Glutamate biosynthetic process
Protein catabolic process in the vacuole

Microtubule depolymerization
Cellular response to hyperoxia
Glycogen metabolic process
Microtubule polymerization
Positive regulation of penicillin metabolic process
Filamentous growth of a population of unicellular organisms in response to starvation
Obsolete GTP catabolic process
Negative regulation of Arp2/3 complex-mediated actin nucleation
Protein import into nucleus
Intracellular protein transport
Mitotic sister chromatid cohesion
Ethanol biosynthetic process involved in glucose fermentation to ethanol
Meiotic nuclear division
Protein folding
Receptor-mediated endocytosis
Nuclear migration along microtubule
Spore germination
Protein polymerization
Negative regulation of transcription during meiosis
Negative regulation of SREBP signaling pathway by positive regulation of TF catabolic process in response to increased oxygen levels

Supplementary Figure 2

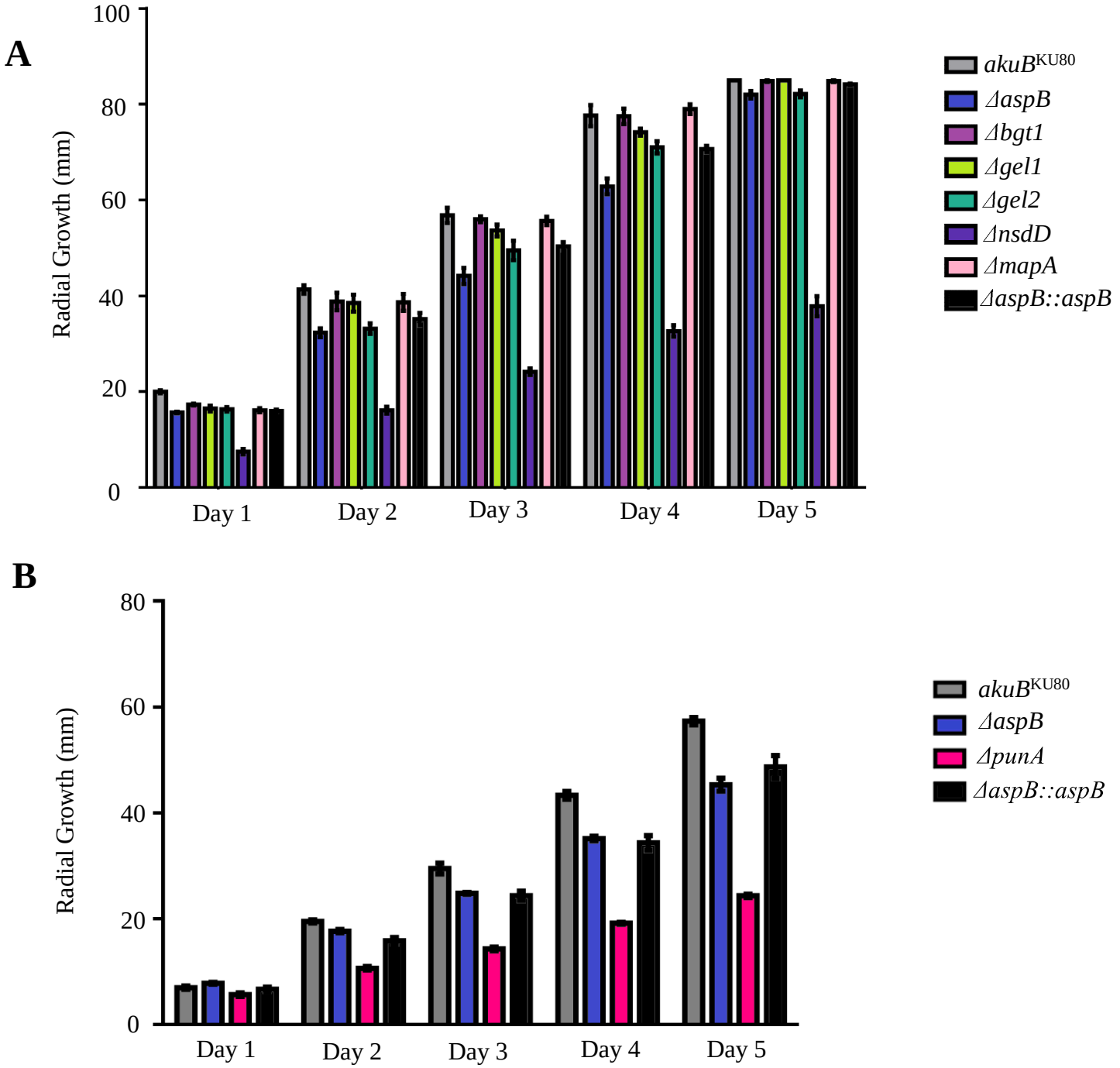

Supplementary Figure 3

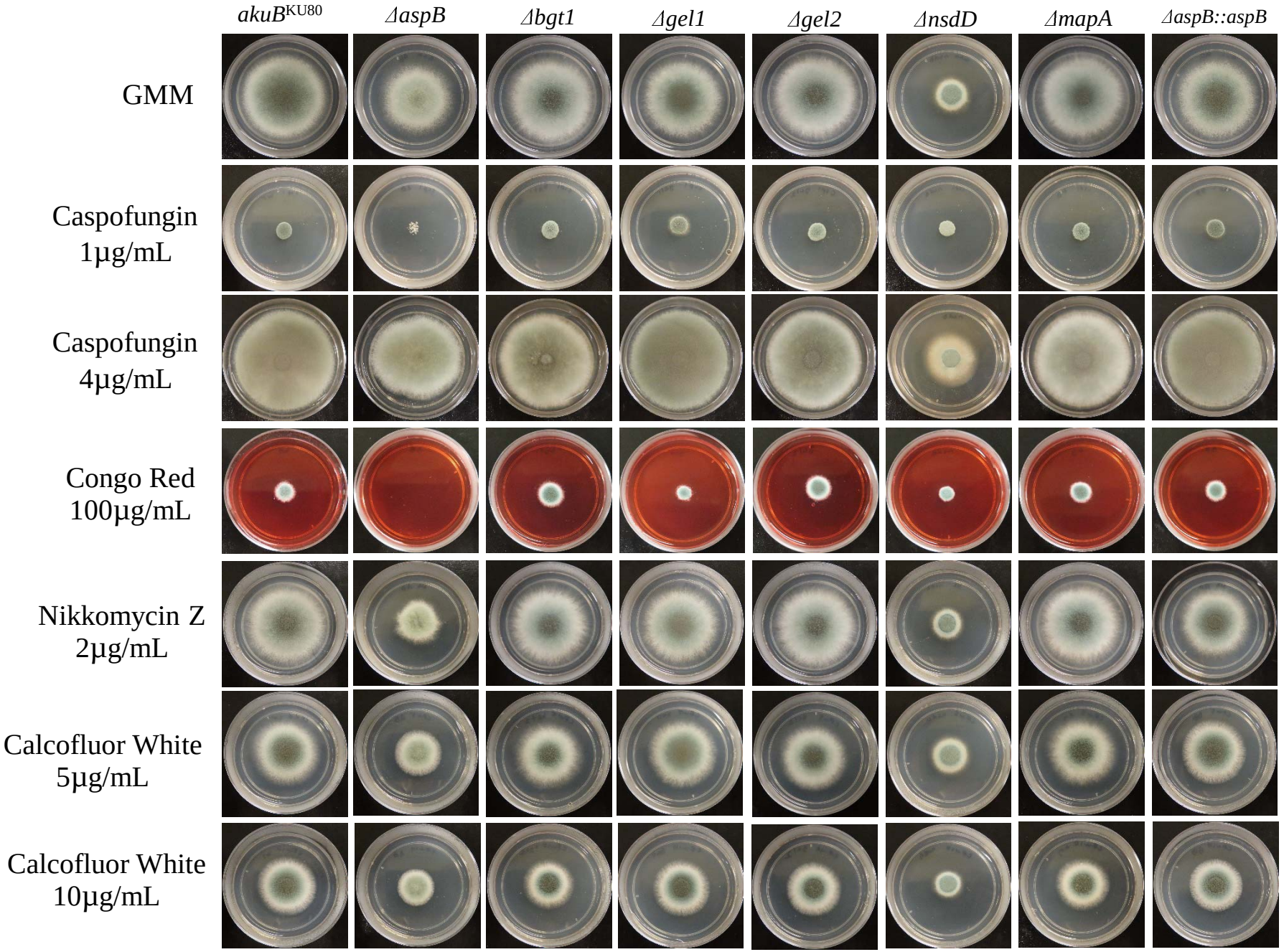

Supplementary Figure 4